Supplemental Information

Control of Platelet CLEC-2-Mediated Activation by Receptor Clustering and Tyrosine Kinase Signaling

Alexey A. Martyanov, Fedor A. Balabin, Joanne L. Dunster, Mikhail A. Panteleev, Jonathan M. Gibbins, and Anastasia N. Sveshnikova

1. Supporting results

1.1. Quiescent state reactions incorporated in our model of CLEC-2-induced platelet activation.

The quiescent state of platelet's tyrosine kinase network is supported by a set of phosphatases, among which CD148 (also known as DEP-1 or PTPRJ) has a dominant role (1–3). Here we assume that SFK can exist in four different states which differ in the degree of activation: non-active SFK (Y527 phosphorylated), a third (1/3) active SFK (Y527 dephosphorylated), two thirds (2/3) active (Y416 phosphorylated) and fully active SFK (Y416 phosphorylated and bound to a phosphorylated tyrosine by its SH-2 domain) (4). Non-active SFK is transferred to the 1/3 active state by active CD148 phosphatases (2, 4). On the contrary, 1/3 active SFK can be deactivated by active Csk kinases, which phosphorylate SFK at Y527 (2, 5). 1/3 active SFK turn to a 2/3 active state via autophosphorylation on Y416 (2). This transition is negatively regulated by the active CD148 (1, 2, 4, 6). We assume that fully active SFK are not produced in the quiescent state due to the absence of the phosphorylated receptor molecules. All types of active SFK mediate phosphorylation of CD148 at Y1311 (6), which results in CD148 activation. On the other side, all types of active SFK also mediate Csk activation (7, 8). It is noteworthy that Csk activation in platelets is not regulated directly by SFK. Namely, SFK phosphorylates a protein called paxillin adapter, which binds Csk and this results in Csk activation (7). Active SFK phosphorylates Syk at Y346, which results in Syk initial activation (9).

It is noteworthy that in *in vivo* experiments with SFK^{-/-} mice CLEC-2 phosphorylation was present upon stimulation by rhodocytin, while further signal propagation was significantly weakened (10). Furthermore, Hughes *et al.* 2015 demonstrated that for CLEC-2 signalling SFK acts mostly as a positive mediator of Syk basal activation (9).

1.2. A detailed description of the model construction in a modular fashion

The "CLEC-2 clustering" module (Fig. 2A) consists of variables for concentrations of CLEC-2 in free, ligand-bound and cluster forms (3 variables, all located in the plasma membrane), fucoidan (1 variable, located in the extracellular space) and 7 parameters, among which 4 concern receptor clustering.

In order to describe cluster formation, we initially used an "N-equation" model (Fig. S1A), which could capture the behavior of the receptor clusters of all sizes (where N is the size of the largest cluster). "N-equation" model of clustering contains 4 parameters: single receptor association and dissociation with clusters rates (k_1, k_{-1}, respectively) and two clusters association and dissociation rates (k_2, k_{-2}, respectively) (11). Formation of clusters of all sizes was described using mass-action kinetics. For example, behaviouor of cluster of size three was described by the following equation:

$$\frac{d[3R]}{dt} = k_1([2R] \times [R] - [3R] \times [R]) + k_{-1}([4R] - [3R]) + k_2([2R] \times [R] - [3R] \times [2R]) + k_{-2}([5R] - [3R]).$$

Average cluster size ($\left. \sum_{i=1}^{n} c_i i \middle/ \sum_{i=1}^{n} c_i \right.$, where c_i – The concentration of the cluster of size i), predicted by the model, was fitted to the data from (12). Calculated distribution of cluster sizes at 300s (Fig. S1C) show that the dimerised receptor concentration is prevailing, while a small fraction of receptors remains in a non-dimerized state.

Although the "N-equation" model could capture the literature data, it was poorly applicable to stochastic calculations. Thus, in order to describe receptor clustering, we utilised a "2-equation model" (13) to describe results obtained by the "N-equation" model.

2-equation model contains 5 parameters, which were determined in the process of fitting the 2-equation model to "N-equation" model, which, in turn, was fitted to experimental data from (12) (for equations and parameter values see Tables S2-S4). Average cluster size was calculated as $s = \left. C_0^* - C^* \middle/ C^{Clust} \right.$, where C_0^* - initial concentration of non-clustered CLEC-2 species, C^* - transient concentration of the non-clustered CLEC-2 and C^{Clust} – transient CLEC-2 cluster concentration.

Both the full model and 2-equation model were capable of accurately simulating available literature data (Fig. S1D). Furthermore, the number of single receptor molecules, predicted by "2-equation" model, corresponded to the value, predicted by "N-equation" model. Based on these results, we considered "2-equation" model applicable for the description of receptor clustering. Thus, "2-equation" model was used in all further calculations.

The "Quiescent state" module (Fig. 2B) of the model consists of variables for concentrations of CD148 phosphatase in active and passive states (2 variables); Csk in active and passive states (2 variables); SFK in a set of gradually active states: non-active, 1/3 active and 2/3 active (3 variables); Syk kinases in active and passive states (2 variables); TULA-2 in active and passive states (2 variables). "Quiescent state" module contains 19 parameters, common with "Tyrosine kinase" module. The initial concentrations of the species (Table S5) were at steady-state values for the module. The "Quiescent state" module was tuned in order to obtain 5% active Syk kinases required for CLEC-2 phosphorylation (9, 10) and 10% of SFKs (Kr^{CD148}, Kr^{Csk}, Kr^{Syk} parameters were estimated). The parameters of the reactions are given in Table S6.

The "Tyrosine kinase" module (Fig. 2C) of the model consists of variables for concentrations of active and inactive Syk kinases (2 variables); SFK in gradually active states: non active, one-third, two-thirds and fully active (4 variables); clustered non phosphorylated and clustered phosphorylated CLEC-2 receptors (2 variables); active and non-active TULA-2 (2 variables).

The unknown parameters of the module (Kr^{CLEC2}, k_{S1}^{SH2}, Kr_{TULA2}^{Syk}, Kf_{Syk}^{TULA2}, Kr_{Syk}^{TULA2}) were estimated by fitting number of active Syk to data from (14), and the number of Y416 phosphorylated SFK to data from (15) (Fig. 2E and S3, correspondingly).

The "LAT-PLCγ2" module (Fig. 2D) consists of variables for concentrations of active Syk (1 variable); phosphorylated and non-phosphorylated LAT (2 variables); LAT-PLCγ2 complexes (1 variable); LAT-PLCγ2-PI3K complexes (1 variable); phosphoinositides (IP$_3$, PIP$_2$ and PIP$_3$, 3 variables); active and non-active Btk (2 variables). The "LAT-PLCγ2" module contains 16 parameters. Unknown parameters (Kr^{LAT}, Kr^{PLC}, k_1^{Btk}, Kr^{PIP_3}) were estimated by fitting numbers of phosphorylated LAT and active PLCγ2 to data from (14) (Fig. 2F and 2G, correspondingly). Initial concentrations of the species in the model and parameter values with equations of the model can be found in tables S7 and S8, correspondingly. The model of Ca^{2+} release (Fig. 2D, "Calcium" module) is described in our previous work (16, 17). It is noteworthy that IP$_3$ concentration in the model of CLEC-2 signalling is a sole link to calcium module and no other positive or negative feedbacks exist in the model. Thus, being the sole generator of IP$_3$, active PLCγ2 was selected as the main output of the model.

2. Supporting Tables.

Table S1. Geometric region details.

Geometric region details			
Name	Parameter	Value	Ref.
The volume of extracellular space	V_{EC}	3.3 µl	(18)
Size of plasmatic membrane	S_{PM}	45 µm^2	(19) Rate of $\frac{S_{PM}}{V_{Cyt}}$ is conserved from (20)
Volume of cytosol	V_{Cyt}	4.5 fl	
Juxtamembrane Volume	V_{JM}	1 fl	An artificial parameter used to preserve dimensions in multi-compartment reactions
Size of the DTS membrane	V_{IM}	1 fl	(19)
The volume of the DTS	V_{DTS}	1.5 fl	

Table S2. "CLEC-2 clustering" module: initial conditions.

Compartment	Species	Variable	Value	Ref.
EC	Ligand	Lig	$2 * 10^{14}$	(14)
PM	Free CLEC-2 molecules	R	2000	(21)
	CLEC-2 molecules, bound to an activator	R^*	0	
	Clustered CLEC-2 molecules	R_C^*	1	

Phosphorylated CLEC-2 molecules	R_P^*		
All clustered CLEC-2 molecules	$R_C = R_P^* + R_C^*$		

Table S3. "CLEC-2 clustering" module: receptor ligation.

Name	Reaction		Equation	Parameters	Ref.
CLEC-2 ligation	M_1	$R + Lig \leftrightarrows R^*$	$S_{PM} \times V_{EC} \times Kf^{Lig} \times Lig \times R$ $- S_{PM} \times Kr^{Lig} \times R^*$	$Kf^{Lig} = 1\ s^{-1} \times \mu mol^{-1}$ $Kr^{Lig} = 0.0302\ s^{-1}$	this work

Table S4. "CLEC-2 clustering" module: receptor clustering description (rapid-receptor dimerisation).

Name	Reaction	Equation	Parameters (ligand-mediated dimerisation)	Parameters (post-ligation dimerisation)	Ref.
Non-clustered CLEC-2	$R^* \leftrightarrows R_C^*$	$\frac{dR^*}{dt}$ $= -k_1 R_C R^* - 2k_2 R^* R^*$ $+ k_{-1} R_C s$	$k_1 = 12324.611\ s^{-1} \times \mu mol^{-1}$ $k_{-1} = 0.0116\ s^{-1} \times \mu mol^{-1}$ $k_2 = 985236\ s^{-1} \times \mu mol^{-1}$	$k_1 = 619.65\ s^{-1} \times \mu mol^{-1}$ $k_{-1} = 0.00205\ s^{-1}$ $k_2 = 8.496\ s^{-1} \times \mu mol^{-1}$	(13)
			s – average cluster size		
Clustered CLEC-2		$\frac{dR_C^*}{dt}$ $= k_2 R^* R^* - k_{-2} R_C R_C + k_3 R_C$	$k_{-2} = 348.26\ s^{-1} \times \mu mol^{-1}$ $k_3 = 2.7 \times 10^{-6}\ s^{-1}$	$k_{-2} = 0.00017\ s^{-1} \times \mu mol^{-1}$ $k_3 = 0.0106\ s^{-1}$	

Table S5. "Tyrosine kinase" and "Quiescent state" module: initial conditions.

Compartment	Species	Variable	Value	Ref.
PM	Non-active SFK (Y527 phosphorylated)	F_P	36800	(22)
	1/3 active SFK	F		
	2/3 active SFK (Y416 phosphorylated)	F^P		
	Active SFK (Y416 phosphorylated, SH2 bound)	F_*^P		
	Non-active CD148	D	3600	
	Active CD148 (Y1311)	D^*		
Cytosol	Non-active Csk	Cs	11500	
	Active Csk	Cs^*		
	Non-active Syk	S	5000	
	Active Syk (Y346 or Y525 phosphorylated)	S^*		
	Non-active TULA-2	T	8000	
	Active TULA-2	T^*		

Table S6. "Tyrosine kinase" and "Quiescent state" module: equations and parameters.

Name	Reaction		Equation	Parameters	Ref.
CD 148 activation	K_1	$D \leftrightarrows D^*$	$S_{PM} \times \left(\frac{\left(\frac{F \times S_{PM}}{V_{JM}} \times kcat_{cat}^{Src}/3 + \frac{F^P \times S_{PM}}{V_{JM}} \times 2 \times kcat_{cat}^{Src}/3 + \frac{F_*^P \times S_{PM}}{V_{JM}} \times kcat_{cat}^{Src} \right)}{Km^{Src} + \frac{D \times S_{PM}}{V_{JM}}} \right) \times D$ $- S_{PM} \times Kr^{CD148} \times D^*$	$k_{cat}^{Src} = 2.1\ s^{-1}$ $Km^{Src} = 3\ \mu M$	(4, 23)
				$Kr^{CD148} = 90.8\ s^{-1}$	*
Csk activation	K_2	$Cs \leftrightarrows Cs^*$	$S_{PM} \times \left(\frac{\left(\frac{F \times S_{PM}}{V_{JM}} \times kcat_{cat}^{Src}/3 + \frac{F^P \times S_{PM}}{V_{JM}} \times 2 \times kcat_{cat}^{Src}/3 + \frac{F_*^P \times S_{PM}}{V_{JM}} \times kcat_{cat}^{Src} \right)}{Km^{Src} + \frac{Cs \times S_{PM}}{V_{JM}}} \right) \times Cs$ $- S_{PM} \times Kr^{CD148} \times Cs^*$	$k_{cat}^{Src} = 2.1\ s^{-1}$ $Km^{Src} = 3\ \mu M$	(4, 23)
				$Kr^{Csk} = 1.0\ s^{-1}$	*
SFK activation 1	K_3	$F_P \leftrightarrows F$	$S_{PM} \times \left(\frac{\frac{D^* \times S_{PM}}{V_{JM}} \times k_{cat}^{CD148}}{Km^{CD148} + \frac{F_P \times S_{PM}}{V_{JM}}} \right) \times F_P - S_{PM} \times \left(\frac{\frac{Cs^* \times S_{PM}}{V_{JM}} \times k_{cat}^{Csk}}{Km^{Csk} + \frac{F \times S_{PM}}{V_{JM}}} \right) \times F$	$k_{cat}^{CD148} = 9.7\ s^{-1}$ $Km^{CD148} = 9.1\ mM$	(24)
				$k_{cat}^{Csk} = 1.9\ s^{-1}$ $Km^{Csk} = 10\ \mu M$	(8)
	K_4	$F \leftrightarrows F^P$		$k_{cat}^{Src} = 2.1\ s^{-1}$ $Km^{Src} = 3\ \mu M$	(4, 23)

Name	Reaction		Equation	Parameters	Ref.
SFK activation 2			$$S_{PM} \times \left(\frac{\left(\frac{F \times S_{PM}}{V_{JM}} \times kcat_{cat}^{Src}/3 + \frac{F^P \times S_{PM}}{V_{JM}} \times 2 \times kcat_{cat}^{Src}/3 + \frac{F_*^P \times S_{PM}}{V_{JM}} \times kcat_{cat}^{Src} \right)}{Km^{Src} + \frac{F \times S_{PM}}{V_{JM}}} \right) \times F \\ - S_{PM} \times \left(\frac{\frac{D^* \times S_{PM}}{V_{JM}} \times k_{cat}^{CD148}}{Km^{CD148} + \frac{F^P \times S_{PM}}{V_{JM}}} \right) \times F^P$$	k_{cat}^{CD148} $= 9.7\ s^{-1}$ Km^{CD148} $= 9.1\ mM$	(24)
SFK activation 3	K_5	$F^P \leftrightarrows F_*^P$	$S_{PM} \times s \times k_{SF1}^{SH2} \times 2 \times R_P^* \times F^P - S_{PM} \times kD_{SFK}^{SH2} \times k_{SF1}^{SH2} \times F_*^P$	s – average cluster size k_{SF1}^{SH2} $= 0.6\ \mu m^2 \times s^{-1}$ $\times \mu mol^{-1}$	*
				kD_{SFK}^{SH2} $= 10^{-6}\ \mu mol/_{\mu m^2}$ $\times s^{-1}$	(25)
TULA-2 activation	K_6	$T \leftrightarrows T^*$	$V_{Cyt} \times Kf_{Syk}^{TULA-2} \times S^* \times T - V_{Cyt} \times Kr_{Syk}^{TULA-2} \times T^*$	Kf_{Syk}^{TULA2} $= 0.1 \mu M^{-1}$ $\times s^{-1}$	*
				Kr_{Syk}^{TULA2} $= 0.007\ s^{-1}$	
CLEC-2 phosphorylation	K_7	$R_C^* \leftrightarrows R_P^*$	$S_{PM} \times \left(\frac{S^* \times k_{cat}^{Syk}}{Km^{Syk} + \frac{R_C^* \times S_{PM}}{V_{JM}}} \right) \times R_C^* - S_{PM} \times Kr^{Phosph} \times R_P^*$	k_{cat}^{Syk} $= 11.85\ s^{-1}$ Km^{Syk} $= 9.1\ \mu M$	(26)
				Kr^{Phosph} $= 0.21\ s^{-1}$	*
Syk activation	K_8	$S \leftrightarrows S^*$	$V_{Cyt} \times \frac{s \times k_{S1}^{SH2} \times S_{PM} \times R_P^*}{V_{JM}} \times \left(\frac{S^* \times k_{cat}^{Syk}}{Km^{Syk} + \frac{S \times S_{PM}}{V_{JM}}} \right) \times S \\ - V_{Cyt} \times \left(kD_{Syk}^{SH2} \times k_{S1}^{SH2} + Kr^{Syk} + Kr_{TULA2}^{Syk} \times T^* \right) \times S^*$	s – average cluster size k_{S1}^{SH2} $= 0.47\ s^{-1}$ $\times \mu M^{-1}$	*
				k_{cat}^{Syk} $= 11.85\ s^{-1}$ Km^{Syk} $= 9.1\ \mu M$	(26)
				kD_{Syk}^{SH2} $= 0.176\ \mu M$	(27)
				$Kr^{Syk} = 10\ s^{-1}$ Kr_{TULA2}^{Syk} $= 7.5\ s^{-1}$ $\times \mu M^{-1}$	*

Table S7. "LAT-PLCγ2" module: initial conditions.

Compartment	Species	Variable	Value	Ref.
PM	LAT	L	4900	(22)
	Phosphorylated LAT	L^*		
	LAT-PLCγ2 complexes	Lp		
	LAT-PLCγ2- PI3K complexes	LP		
	PIP$_2$	I_1	200 µM	(19)
	PIP$_3$	I_2		
	Active Btk	B^*	0	(22)
	Active PLCγ2	p^*		
Cytosol	Non-active PI3K	P	1900	
	Non-active PLCγ2	p	2000	
	Non-active Btk	B	11100	
	IP$_3$	I_3	0.05 nM	(19)

Table S8. "LAT-PLCγ2" module: equations and parameters.

Name	Reaction		Equation	Parameters	Ref.
LAT phosphoryl	PL_1	$L \leftrightarrows L^*$		$k_{cat}^{Syk} = 11.85\ s^{-1}$ $Km^{Syk} = 9.1\ \mu M$	(4, 23)

			Rate equation	Parameters	Ref
ation by Syk			$S_{PM} \times \left(\dfrac{S^* \times k_{cat}^{Syk}}{Km^{Syk} + \frac{L \times S_{PM}}{V_{JM}}} \right) \times L - S_{PM} \times Kr^{LAT} \times (L^* + Lp + LP + p^*)$	$Kr^{LAT} = 1.41\ s^{-1}$	*
LAT-PLCγ2 complex formation	PL_2	$p \leftrightarrows Lp$	$S_{PM} \times k_1^{Lp} \times L^* \times p - S_{PM} \times kD_{Lp} \times k_1^{Lp} \times (Lp + LP + p^*)$	$k_1^{Lp} = 0.9\mu M^{-1} \times s^{-1}$	*
				$kD_{Lp} = 0.15\ \mu M$	(25)
LAT-PLCγ2-PI3K complex formation	PL_3	$P \leftrightarrows LP$	$S_{PM} \times k_1^{LP} \times Lp \times P - S_{PM} \times kD_{LP} \times k_1^{LP} \times LP$	$k_1^{LP} = 4.2\ \mu M^{-1} \times s^{-1}$	*
				$kD_{LP} = 0.22\ \mu M$	(25)
PIP₃ production	PL_4	$I_1 \leftrightarrows I_2$	$S_{PM} \times \left(\dfrac{\frac{LP \times S_{PM}}{V_{JM}} \times k_{cat}^{PI3K}}{Km^{PI3K} + \frac{I_1 \times S_{PM}}{V_{JM}}} \right) \times I_1 - S_{PM} \times Kr^{PIP_3} \times (I_2 + B^*)$	$k_{cat}^{PI3K} = 2.82\ s^{-1}$	*
				$Km^{PI3K} = 11\ \mu M$	(19)
				$Kr^{PIP_3} = 0.44\ s^{-1}$	*
Btk activation	PL_5	$B \leftrightarrows B^*$	$S_{PM} \times k_1^{BI} \times I_2 \times B - S_{PM} \times kD_{BI} \times k_1^{BI} \times B^*$	$k_1^{BI} = 0.51\ \mu M^{-1} \times s^{-1}$	*
				$kD_{BI} = 0.64\ \mu M$	(25)
PLCγ2 activation	PL_6	$Lp \leftrightarrows p^*$	$S_{PM} \times \left(\dfrac{\frac{B^* \times S_{PM}}{V_{JM}} \times k_{cat}^{Btk}}{Km^{Btk} + \frac{Lp \times S_{PM}}{V_{JM}}} \right) \times Lp - S_{PM} \times Kr^{PLC} \times p^*$	$k_{cat}^{Btk} = 0.14\ s^{-1}$	(4, 28)
				$Km^{Btk} = 37\ \mu M$	
				$Kr^{PLC} = 8.6 \times 10^{-3}\ s^{-1}$	*
IP₃ production	PL_7	$I_1 \leftrightarrows I_3$	$S_{PM} \times \left(\dfrac{\frac{p^* \times S_{PM}}{V_{JM}} \times k_{cat}^{PLC\gamma2} \times (Ca)}{Km^{PLC\gamma2} + (Ca)} \right) \times I_1 - V_{Cyt} \times Kr^{IP_3} \times I_3$	$k_{cat}^{PLC\gamma2} = 30.5\ s^{-1}$	*
				$Km^{PLC\gamma2} = 0.78\ \mu M$	
				$Kr^{IP_3} = 60\ s^{-1}$	

Detailed calcium module description is given in (19).

Table S9. Models in COPASI Software.

Model of platelet CLEC-2 induced activation with rapid, ligand-induced receptor dimerisation	CLEC2_rapidclust.xml
Model of platelet CLEC-2 induced activation with post-ligation receptor dimerisation	CLEC2_altclust.xml

Table S10. Sensitivity scores of the most influential parameters for the number of active Syk kinases at the point of maximal activation.

Module	Parameter name	Variable	Value	Variation limits	Sensitivity Score
"CLEC-2 clustering" module	CLEC-2 clustering: k_{-2}	k_{-2}	$348.26\ s^{-1} \times \mu mol^{-1}$	$25 - 250$	0.077
	CLEC-2 clustering: k_{-1}	k_{-1}	$0.0116\ s^{-1} \times \mu mol^{-1}$	$0.001 - 0.01$	0.044
	CLEC-2 clustering: k_1	k_1	$12324.611\ s^{-1} \times \mu mol^{-1}$	$5000 - 50000$	0.014
"Tyrosine kinase" module	the forward rate of Syk activation by SH-2 domains	k_{S1}^{SH2}	$0.47\ s^{-1} \times \mu M^{-1}$	$0.2 - 2$	1.21245
	reverse rate of CLEC-2 phosphorylation	Kr^{Phosph}	$0.21\ s^{-1}$	$0.05 - 0.5$	1.10722
	the turnover rate of Syk kinases	k_{cat}^{Syk}	$11.85\ s^{-1}$	$5 - 15$	1.10362
	Michaelis constant of Syk kinases	Km^{Syk}	$9.1\ \mu M$	$5 - 15$	0.997198

	Parameter name	Variable	Value	Variation limits	Sensitivity Score
	reverse rate of Syk activation by SFK kinases	Kr^{Syk}	$10\ s^{-1}$	$5-25$	0.775836
	Syk deactivation by TULA-2 rate	Kr^{Syk}_{TULA2}	$7.5\ s^{-1} \times \mu M^{-1}$	$2-20$	0.734043
	the forward rate of TULA-2 activation by Syk	Kf^{TULA2}_{Syk}	$0.1 \mu M^{-1} \times s^{-1}$	0.05 - 0.5	0.559938
	reverse rate of TULA-2 activation by Syk	Kr^{TULA2}_{Syk}	$0.007\ s^{-1}$	0.01 - 0.1	0.21001
	the turnover rate of SFK kinases	k^{Src}_{cat}	$2.1\ s^{-1}$	$0.5-5$	0.17258
	Michaelis constant of CD148	Km^{CD148}	$9.1\ mM$	4550 - 18200	0.010652
	reverse rate of CD148 activation	Kr^{CD148}	$90.8\ s^{-1}$	40 - 200	0.010623
	the turnover rate of CD148	k^{CD148}_{cat}	$9.7\ s^{-1}$	4 - 20	0.010536
	Syk initial number	S	5000	2500 - 10000	1.46352
	TULA-2 initial number	T	8000	3750 - 15000	0.680195
	SFK initial number	F_P	36800	10000 - 40000	0.010381
Comp. Sizes	platelet cytosol volume	V_{Cyt}	$4.5\ fl$	$2.25-9$	1
	plasma membrane area	S_{PM}	$45\ \mu m^2$	25 - 90	0.152712

Table S11. Sensitivity scores of the most influential parameters for the number of phosphorylated LAT at the point of maximal activation.

Module	Parameter name	Variable	Value	Variation limits	Sensitivity Score
"CLEC-2 clustering" module	CLEC-2 clustering: k₋₂	k_{-2}	$348.26\ s^{-1} \times \mu mol^{-1}$	$25-250$	0.080092
	CLEC-2 clustering: k₋₁	k_{-1}	$0.0116\ s^{-1} \times \mu mol^{-1}$	$0.001-0.01$	0.035984
	CLEC-2 clustering: k₁	k_1	$12324.611\ s^{-1} \times \mu mol^{-1}$	$5000 - 50000$	0.01352
	CLEC-2 initial number	R	2000	1000-4000	0.061893
"Tyrosine kinase" module	turnover rate of Syk kinases	k^{Syk}_{cat}	$11.85\ s^{-1}$	$5-15$	2.34692
	Michaelis constant of Syk kinases	Km^{Syk}	$9.1\ \mu M$	$5-15$	1.71089
	the forward rate of Syk activation by SH-2 domains	k^{SH2}_{S1}	$0.47\ s^{-1} \times \mu M^{-1}$	$0.2-2$	1.53089
	reverse rate of Syk activation by SFK kinases	Kr^{Syk}	$10\ s^{-1}$	$5-25$	1.37626
	reverse rate of CLEC-2 phosphorylation	Kr^{Phosph}	$0.21\ s^{-1}$	0.05 - 0.5	1.07892

	Syk deactivation by TULA-2 rate	Kr_{TULA2}^{Syk}	$7.5\ s^{-1} \times \mu M^{-1}$	2 – 20	0.531341
	the forward rate of TULA-2 activation by Syk	Kf_{Syk}^{TULA2}	$0.1 \mu M^{-1} \times s^{-1}$	0.05 - 0.5	0.348428
	the turnover rate of SFK kinases	k_{cat}^{Src}	$2.1\ s^{-1}$	0.5-5	0.136494
	reverse rate of TULA-2 activation by Syk	Kr_{Syk}^{TULA2}	$0.007\ s^{-1}$	0.01 - 0.1	0.05687
	Syk SH-2 domains kD	kD_{Syk}^{SH2}	$0.176\ \mu M$	0.05-0.5	0.011793
	Syk initial number	S	5000	2500 - 10000	1.91275
	TULA-2 initial number	T	8000	3750 - 15000	0.369641
"LAT-PLCγ2" module	reverse rate of LAT phosphorylation	Kr^{LAT}	$1.41\ s^{-1}$	0.25 - 2.5	0.983638
	LAT initial number	L	4900	2500 - 10000	0.544366
Comp. Sizes	plasma membrane area	S_{PM}	$45\ \mu m^2$	25 - 90	0.39402

Table S12. Sensitivity scores of the most influential parameters for the number of active PLCγ2 at point of maximal activation.

Module	Parameter name	Variable	Value	Variation limits	Sensitivity Score
"CLEC-2 clustering" module	CLEC-2 clustering: k-2	k_{-2}	$348.26\ s^{-1} \times \mu mol^{-1}$	25 – 250	0.129158
	CLEC-2 clustering: k-1	k_{-1}	$0.0116\ s^{-1} \times \mu mol^{-1}$	0.001 – 0.01	0.062745
	CLEC-2 clustering: k1	k_1	$12324.611\ s^{-1} \times \mu mol^{-1}$	5000 – 50000	0.021921
	CLEC-2 clustering: k3	k_3	$2.7 \times 10^{-6}\ s^{-1}$	0.0001 – 0.001	0.011867
	CLEC-2 initial number	R	2000	1000-4000	0.08554
"Tyrosine kinase" module	turnover rate of Syk kinases	k_{cat}^{Syk}	$11.85\ s^{-1}$	5 – 15	3.86148
	Michaelis constant of Syk kinases	Km^{Syk}	$9.1\ \mu M$	5 – 15	2.8085
	the forward rate of Syk activation by SH-2 domains	k_{S1}^{SH2}	$0.47\ s^{-1} \times \mu M^{-1}$	0.2 – 2	2.38768
	reverse rate of Syk activation by SFK kinases	Kr^{Syk}	$10\ s^{-1}$	5 – 25	2.0621
	reverse rate of CLEC-2 phosphorylation	Kr^{Phosph}	$0.21\ s^{-1}$	0.05 - 0.5	1.78911
	Syk deactivation by TULA-2 rate	Kr_{TULA2}^{Syk}	$7.5\ s^{-1} \times \mu M^{-1}$	2 – 20	0.993338
	the forward rate of TULA-2 activation by Syk	Kf_{Syk}^{TULA2}	$0.1 \mu M^{-1} \times s^{-1}$	0.05 - 0.5	0.681899
	the turnover rate of SFK kinases	k_{cat}^{Src}	$2.1\ s^{-1}$	0.5-5	0.262073

	reverse rate of TULA-2 activation by Syk	Kr_{Syk}^{TULA2}	$0.007\ s^{-1}$	0.01 - 0.1	0.16055
	Syk SH-2 domains kD	kD_{Syk}^{SH2}	$0.176\ \mu M$	0.05-0.5	0.0173905
	Syk initial number	S	5000	2500 - 10000	3.00666
	TULA-2 initial number	T	8000	3750 - 15000	0.765108
"LAT-PLCγ2" module	reverse rate of LAT phosphorylation	Kr^{LAT}	$1.41\ s^{-1}$	0.25 - 2.5	1.6537
	the turnover rate of Btk	k_{cat}^{Btk}	$0.14\ s^{-1}$	0.07 - 0.28	0.795997
	Michaelis constant of Btk	Km^{Btk}	$37\ \mu M$	18 - 74	0.793626
	the turnover rate of PI3K	k_{cat}^{PI3K}	$2.82\ s^{-1}$	1.4 - 5.65	0.70601
	reverse rate of PIP$_3$ production by PI3K	Kr^{PIP_3}	$0.44\ s^{-1}$	0.2 - 0.9	0.691281
	reverse rate of PLCγ2 activation	Kr^{PLC}	$8.6 \times 10^{-3}\ s^{-1}$	0.005 - 0.05	0.260846
	PLCγ2 kD from phosphorylated LAT	kD_{Lp}	$0.15\ \mu M$	0.075 - 0.3	0.146303
	Michaelis constant of PI3K	Km^{PI3K}	$11\ \mu M$	5.5 - 22	0.0369431
	the forward rate of Btk activation upon PIP$_3$ binding	k_1^{BI}	$0.51\ \mu M^{-1} \times s^{-1}$	0.25 - 1	0.0113054
	PI3K kD from phosphorylated LAT	kD_{LP}	$0.22\ \mu M$	0.11 - 0.44	0.0108299
	LAT initial number	L	4900	2500 - 10000	0.912258
	Btk initial number	B	11100	5000 - 25000	0.796234
	PLCγ2 initial number	p	2000	1000 - 4000	0.152649
	PI3K initial number	P	1900	950 - 3800	0.0115858
Comp. Sizes	plasma membrane area	S_{PM}	$45\ \mu m^2$	25 - 90	0.73603

Table S13. Sensitivity scores of the most influential parameters for the IP$_3$ concentration at the point of maximal activation.

Module	Parameter name	Variable	Value	Variation limits	Sensitivity Score
"CLEC-2 clustering" module	CLEC-2 clustering: k$_{-2}$	k_{-2}	$348.26\ s^{-1} \times \mu mol^{-1}$	25 – 250	0.190352
	CLEC-2 clustering: k$_{-1}$	k_{-1}	$0.0116\ s^{-1} \times \mu mol^{-1}$	0.001 – 0.01	0.092191
	CLEC-2 clustering: k$_1$	k_1	$12324.611\ s^{-1} \times \mu mol^{-1}$	5000 – 50000	0.032406
	CLEC-2 clustering: k$_3$	k_3	$2.7 \times 10^{-6}\ s^{-1}$	0.0001 – 0.001	0.0175
	CLEC-2 initial number	R	2000	1000-4000	0.126508
	turnover rate of Syk kinases	k_{cat}^{Syk}	$11.85\ s^{-1}$	5 – 15	5.71225

"Tyrosine kinase" module	Michaelis constant of Syk kinases	Km^{Syk}	$9.1\ \mu M$	$5-15$	4.12844
	the forward rate of Syk activation by SH-2 domains	k_{S1}^{SH2}	$0.47\ s^{-1} \times \mu M^{-1}$	$0.2-2$	3.52858
	reverse rate of Syk activation by SFK kinases	Kr^{Syk}	$10\ s^{-1}$	$5-25$	3.03843
	reverse rate of CLEC-2 phosphorylation	Kr^{Phosph}	$0.21\ s^{-1}$	0.05 - 0.5	2.6302
	Syk deactivation by TULA-2 rate	Kr_{TULA2}^{Syk}	$7.5\ s^{-1} \times \mu M^{-1}$	$2-20$	1.45979
	the forward rate of TULA-2 activation by Syk	Kf_{Syk}^{TULA2}	$0.1 \mu M^{-1} \times s^{-1}$	0.05 - 0.5	1.00145
	the turnover rate of SFK kinases	k_{cat}^{Src}	$2.1\ s^{-1}$	0.5-5	0.386137
	reverse rate of TULA-2 activation by Syk	Kr_{Syk}^{TULA2}	$0.007\ s^{-1}$	0.01 - 0.1	0.235098
	Syk SH-2 domains kD	kD_{Syk}^{SH2}	$0.176\ \mu M$	0.05-0.5	0.025556
	reverse rate of CD148 activation	Kr^{CD148}	$90.8\ s^{-1}$	40 - 200	0.011223
	the turnover rate of CD148	k_{cat}^{CD148}	$9.7\ s^{-1}$	4 - 20	0.010769
	Michaelis constant of CD148	Km^{CD148}	$9.1\ mM$	4550 - 18200	0.010616
	Syk initial number	S	5000	2500 - 10000	4.44675
	TULA-2 initial number	T	8000	3750 - 15000	1.12288
	SFK initial number	F_P	36800	10000 - 40000	0.010622
"LAT-PLCγ2" module	reverse rate of LAT phosphorylation	Kr^{LAT}	$1.41\ s^{-1}$	0.25 - 2.5	2.43175
	reverse rate of IP$_3$ production	Kr^{IP_3}	$60\ s^{-1}$	$20-100$	1.47202
	the turnover rate of Btk	k_{cat}^{Btk}	$0.14\ s^{-1}$	0.07 - 0.28	1.17565
	Michaelis constant of Btk	Km^{Btk}	$37\ \mu M$	18 - 74	1.17029
	the turnover rate of PI3K	k_{cat}^{PI3K}	$2.82\ s^{-1}$	1.4 - 5.65	1.03907
	reverse rate of PIP$_3$ production by PI3K	Kr^{PIP_3}	$0.44\ s^{-1}$	0.2 - 0.9	1.01565
	reverse rate of PLCγ2 activation	Kr^{PLC}	$8.6 \times 10^{-3}\ s^{-1}$	0.005 - 0.05	0.382328
	PLCγ2 kD from phosphorylated LAT	kD_{Lp}	$0.15\ \mu M$	0.075 - 0.3	0.215728
	Michaelis constant of PI3K	Km^{PI3K}	$11\ \mu M$	5.5 - 22	0.054275
	the forward rate of Btk activation upon PIP$_3$ binding	k_1^{BI}	$0.51\ \mu M^{-1} \times s^{-1}$	0.25 - 1	0.016936

	PI3K kD from phosphorylated LAT	kD_{LP}	0.22 μM	0.11 - 0.44	0.015487
	LAT initial number	L	4900	2500 - 10000	1.3449
	Btk initial number	B	11100	5000 - 25000	1.17598
	PLCγ2 initial number	p	2000	1000 - 4000	0.225426
	PI3K initial number	P	1900	950 - 3800	0.016803
Comp. Sizes	plasma membrane area	S_{PM}	45 μm^2	25 - 90	2.70157

Table S14. Sensitivity scores of the most influential parameters for the calcium concentration at the point of maximal activation.

	k_1; $s^{-1} \times \mu mol^{-1}$	k_{-2}; $s^{-1} \times \mu mol^{-1}$	k_3; s^{-1}
37ºC	13924.4	348.26	2.7×10^{-6}
25ºC	2249	251.16	1.8×10^{-6}
25ºC, 1mM mβCD	164	208.07	1×10^{-6}

Table S15. "CLEC-2 clustering" module parameters, corresponding to different activatory conditions.

System of differential equations corresponding to the biochemical reactions incorporated in the stochastic model:

$$\frac{dLig}{dt} \times V_{EC} = -M_1 \tag{1}$$

$$\frac{dR}{dt} \times S_{PM} = -M_1 \tag{2}$$

$$\frac{dR^*}{dt} \times S_{PM} = M_1 + TS5_1 \tag{3}$$

$$\frac{dR_C^*}{dt} \times S_{PM} = TS5_2 - K_7 \tag{4}$$

$$\frac{dR_P^*}{dt} \times S_{PM} = K_7 \tag{5}$$

$$\frac{dD}{dt} \times S_{PM} = -K_1 \tag{6}$$

$$\frac{dD^*}{dt} \times S_{PM} = K_1 \tag{7}$$

$$\frac{dCs}{dt} \times V_{Cyt} = -K_2 \tag{8}$$

$$\frac{dCs^*}{dt} \times V_{Cyt} = K_2 \tag{9}$$

$$\frac{dF_P}{dt} \times S_{PM} = -K_3 \tag{10}$$

$$\frac{dF}{dt} \times S_{PM} = K_3 - K_4 \tag{11}$$

$$\frac{dF^P}{dt} \times S_{PM} = K_4 - K_5 \tag{12}$$

$$\frac{dF_*^P}{dt} \times S_{PM} = K_5 \tag{13}$$

$$\frac{dT}{dt} \times V_{Cyt} = -K_6 \tag{14}$$

$$\frac{dT^*}{dt} \times V_{Cyt} = K_6 \tag{15}$$

$$\frac{dS}{dt} \times V_{Cyt} = -K_8 \tag{16}$$

$$\frac{dS^*}{dt} \times V_{Cyt} = K_8 \tag{17}$$

$$\frac{dL}{dt} \times S_{PM} = -PL_1 \tag{18}$$

$$\frac{dL^*}{dt} \times S_{PM} = PL_1 \tag{19}$$

$$\frac{dLp}{dt} \times S_{PM} = PL_2 - PL_6 \tag{20}$$

$$\frac{dLP}{dt} \times S_{PM} = PL_3 \tag{21}$$

$$\frac{dp}{dt} \times V_{Cyt} = -PL_2 \tag{22}$$

$$\frac{dP}{dt} \times V_{Cyt} = -PL_3 \tag{23}$$

$$\frac{dI_1}{dt} \times S_{PM} = -PL_4 - PL_7 \tag{24}$$

$$\frac{dI_2}{dt} \times S_{PM} = PL_4 \tag{25}$$

$$\frac{dB}{dt} \times V_{Cyt} = -PL_5 \tag{26}$$

$$\frac{dB^*}{dt} \times S_{PM} = PL_5 \tag{27}$$

$$\frac{dp^*}{dt} \times S_{PM} = PL_6 \tag{28}$$

$$\frac{dI_3}{dt} \times V_{Cyt} = PL_7 \tag{29}$$

3. Supporting Figures
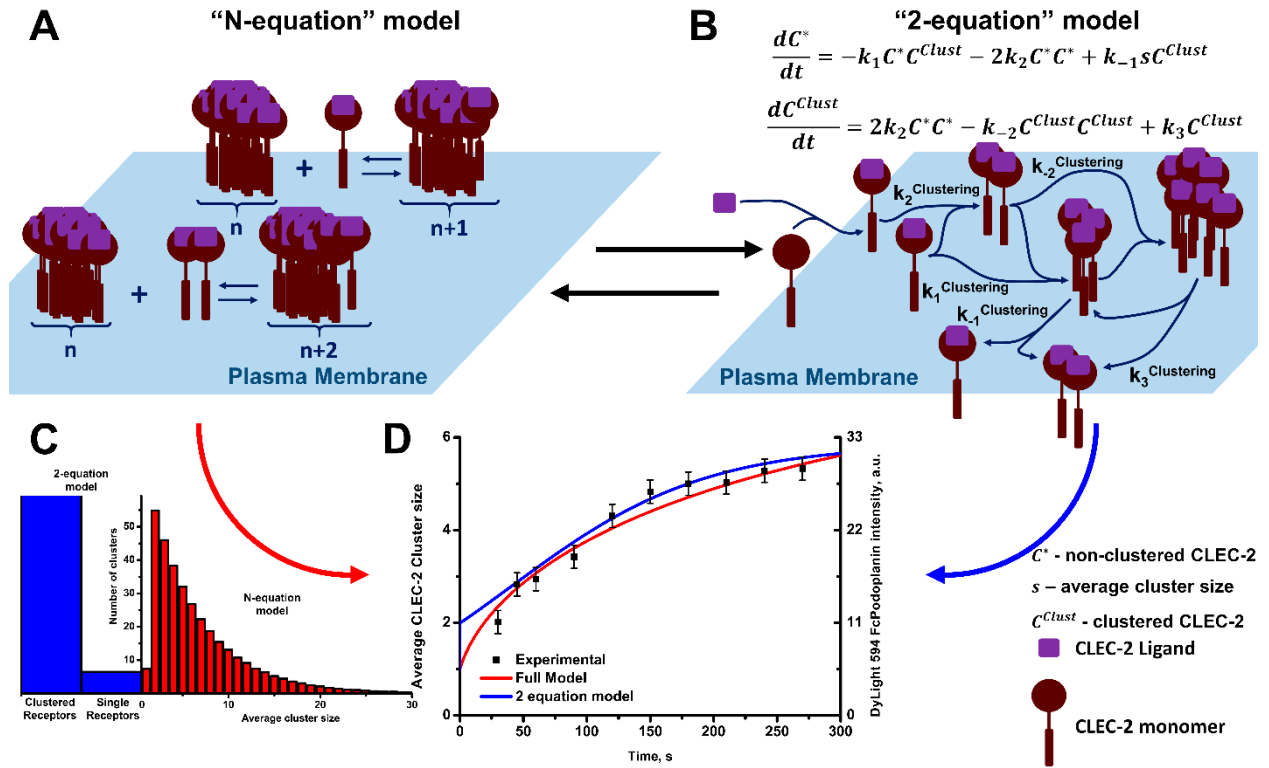
Figure S1. CLEC-2 receptor clustering models. In order to describe platelet CLEC-2 receptor clustering two approaches were used: N-equation model of receptor clustering, which describes behavior of the clusters of the receptors of each size explicitly (A – scheme, C- average cluster size) – (11) and 2-equation model, that describes behavior of the receptor clusters in general (B) – (13). Both models were capable of describing experimental data showing the clustering of CLEC-2, calculated from absolute fluorescent intensity data (12) under the assumption that only CLEC-2 monomers and dimers are present on the surface of resting platelets (29) (D). More simplistic approach – 2-equation model – was used for the construction of the complete model of CLEC-2 signalling, because it both allowed to describe experimental data and to reduce computational complexity.
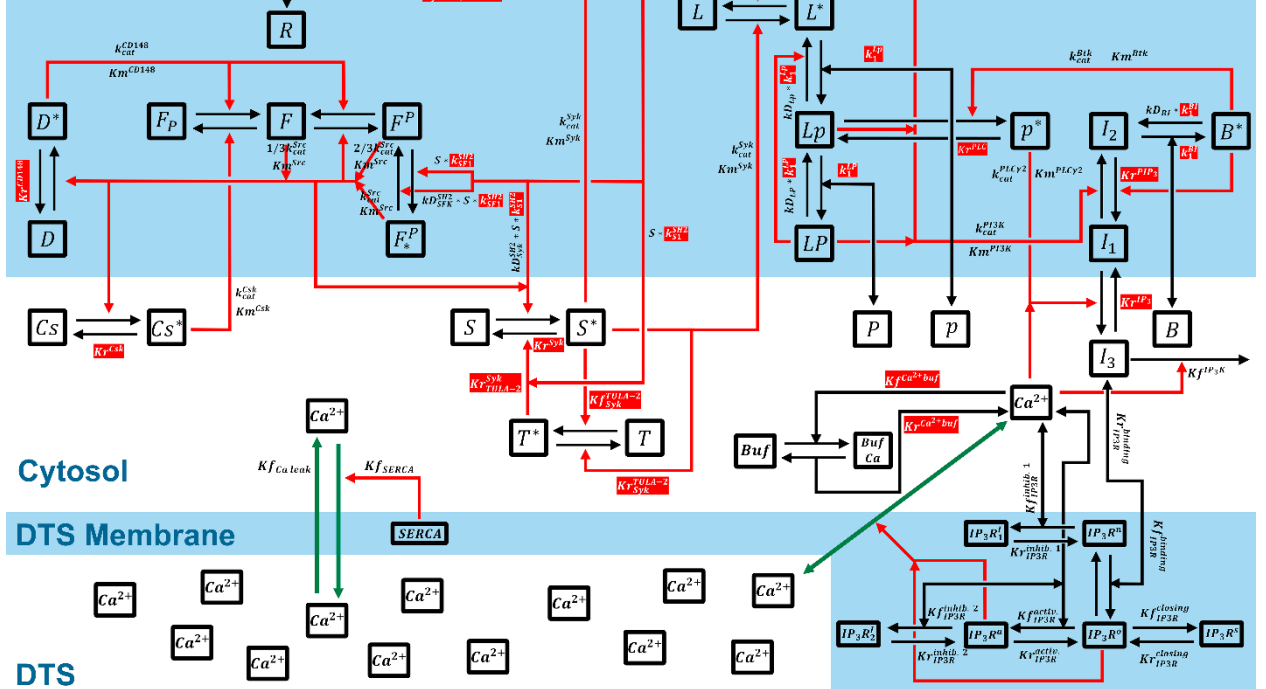
Figure S2. Network diagram of the platelet CLEC-2 signalling model. Black lines represent transitions between the different state of the incorporated species. Red lines represent catalysis. Green lines represent calcium ions transitions from DTS to the cytosol. Unknown parameter values are highlighted in red. All parameter values can be found in Supplementary Tables S4,5,7,9.
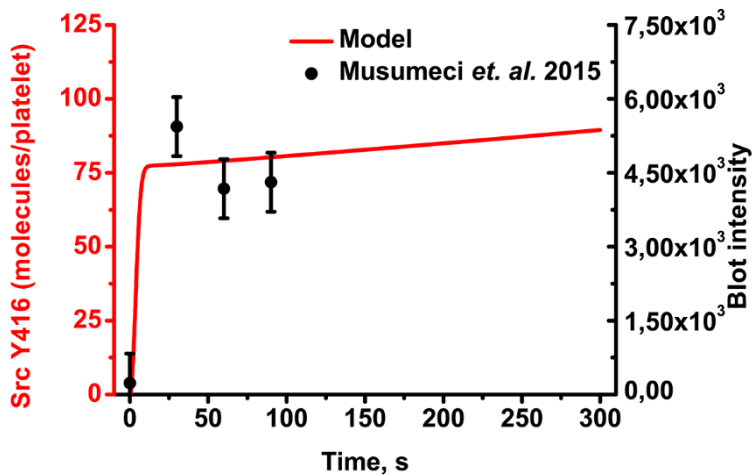
Figure S3. Model validation. Comparison of the numbers of Y416 phosphorylated amount of SFK predicted by the model to experimental data available from the literature (15).

14

Ligand mediated receptor dimerisation

Post-ligation receptor dimerisation
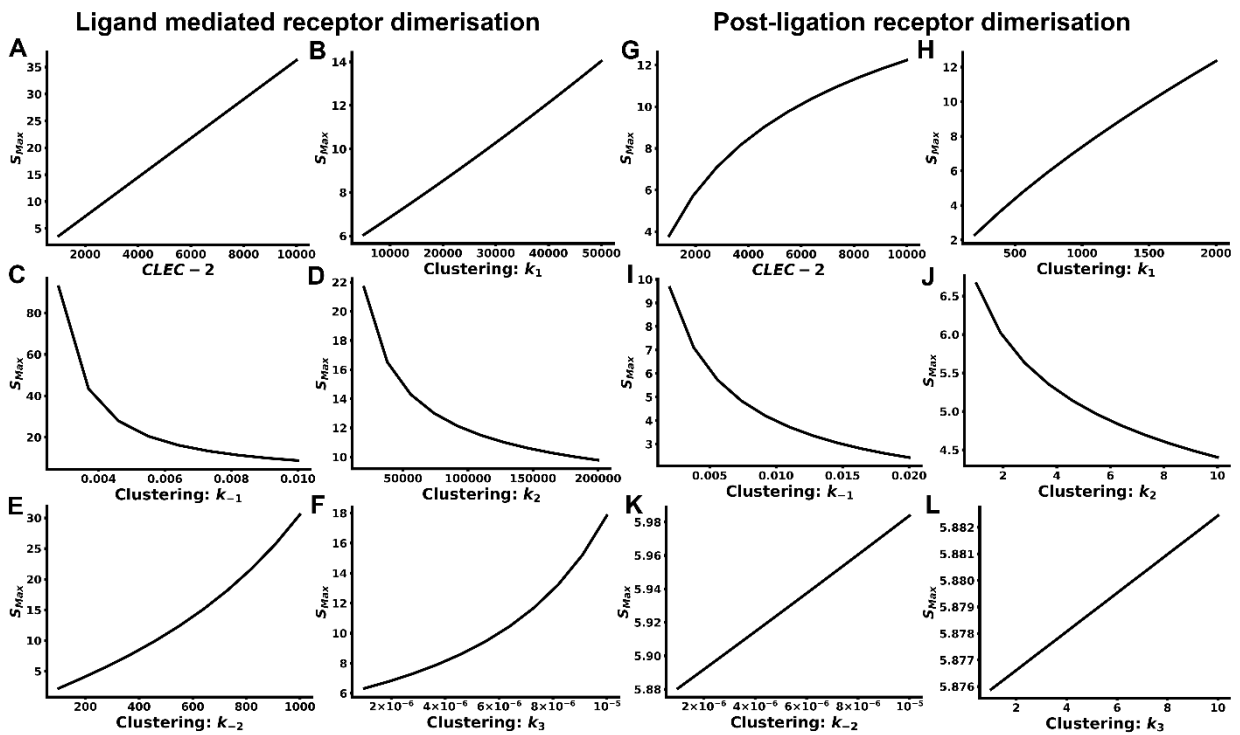
Figure S4. Explicit variation of the parameters of the "CLEC-2 clustering module". (A-C) Impact of the "CLEC-2 clustering" parameters on maximal CLEC-2 cluster size (S_{Max}) in "Ligand mediated receptor dimerisation" mode: CLEC-2 initial number (A), CLEC-2 clustering k_1 (B), CLEC-2 clustering k_{-1} (C), CLEC-2 clustering k_2 (D), CLEC-2 clustering k_{-2} (E), CLEC-2 clustering k_3 (F). (G-L) Impact of the "CLEC-2 clustering" parameters on maximal CLEC-2 cluster size (S_{Max}) in "Ligand mediated receptor dimerisation" mode: CLEC-2 initial number (G), CLEC-2 clustering k_1 (H), CLEC-2 clustering k_{-1} (I), CLEC-2 clustering k_2 (J), CLEC-2 clustering k_{-2} (K), CLEC-2 clustering k_3 (L).
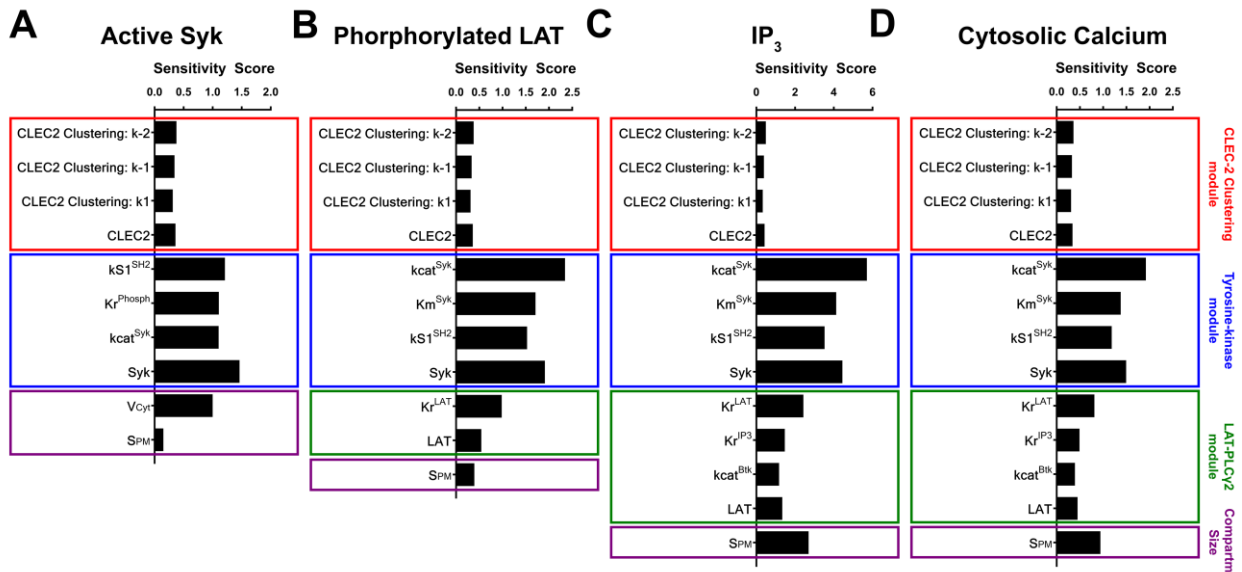
Figure S5. Local sensitivity analysis. Sensitivity score of the most influential parameters from each of the module and the most influential initial concentration, concerning: number of active Syk kinases (A), number of phosphorylated LAT (B), IP_3 concentration (C), cytosolic calcium concentration (D). Red colour highlights "CLEC-2 clustering" module, blue – "Tyrosine kinase" module, green – "LAT-PLCγ2" module, purple – initial volumes of the model compartments.

15
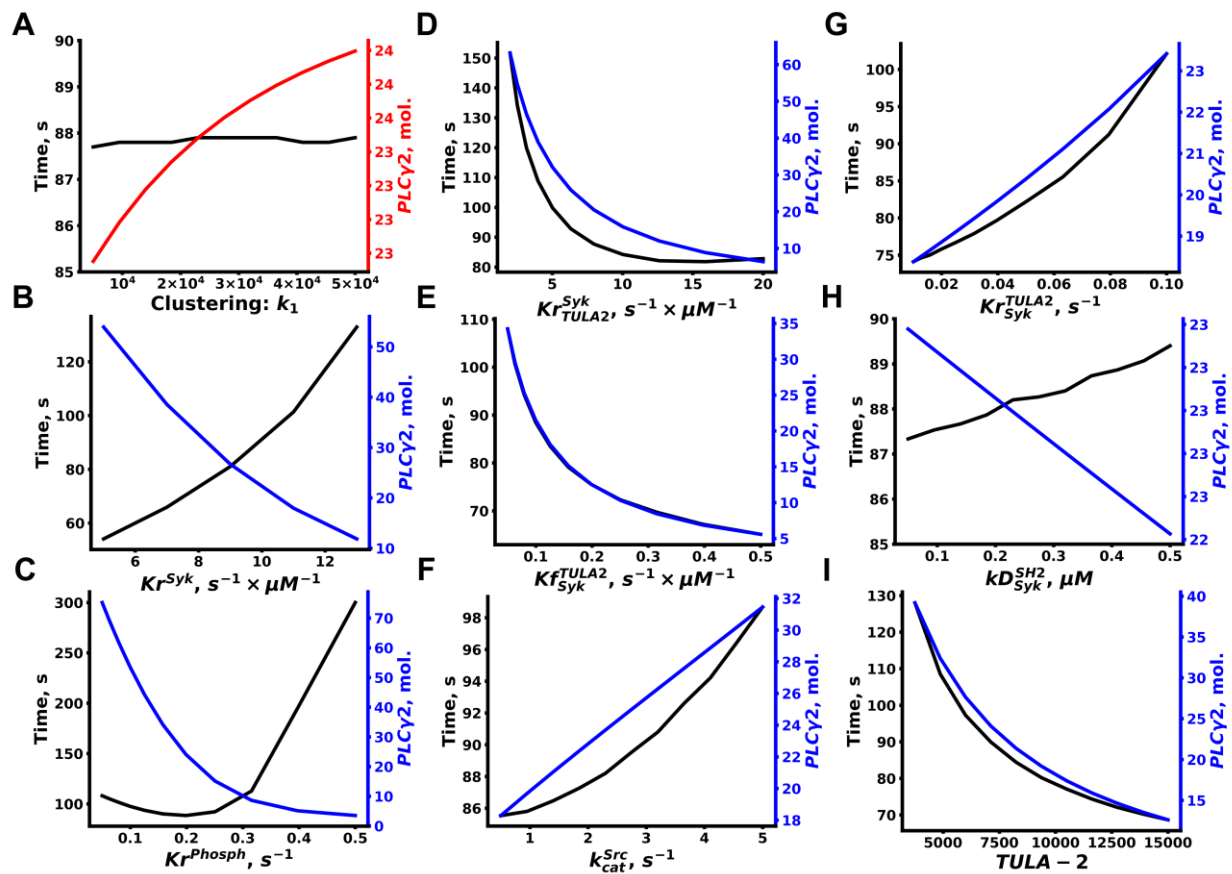
Figure S6. Explicit variation of the parameters with the sensitivity score above 0.01 for effect on maximal amount of active PLCγ2 and time to maximum (from CLEC-2 clustering k_1 to TULA-2 initial concentration). CLEC-2 clustering k_1 (A), reverse rate of Syk activation by SFK kinases (B), reverse rate of CLEC-2 phosphorylation (C), Syk deactivation by TULA-2 rate (D), forward rate of TULA-2 activation by Syk (E), turnover rate of SFK kinases (F), reverse rate of TULA-2 activation by Syk (G), Syk SH-2 domains kD from phosphorylated tyrosine residues in hemITAM sequences (H), TULA-2 initial number (I). Red colour highlights "CLEC-2 clustering" module, blue – "Tyrosine kinase" module.
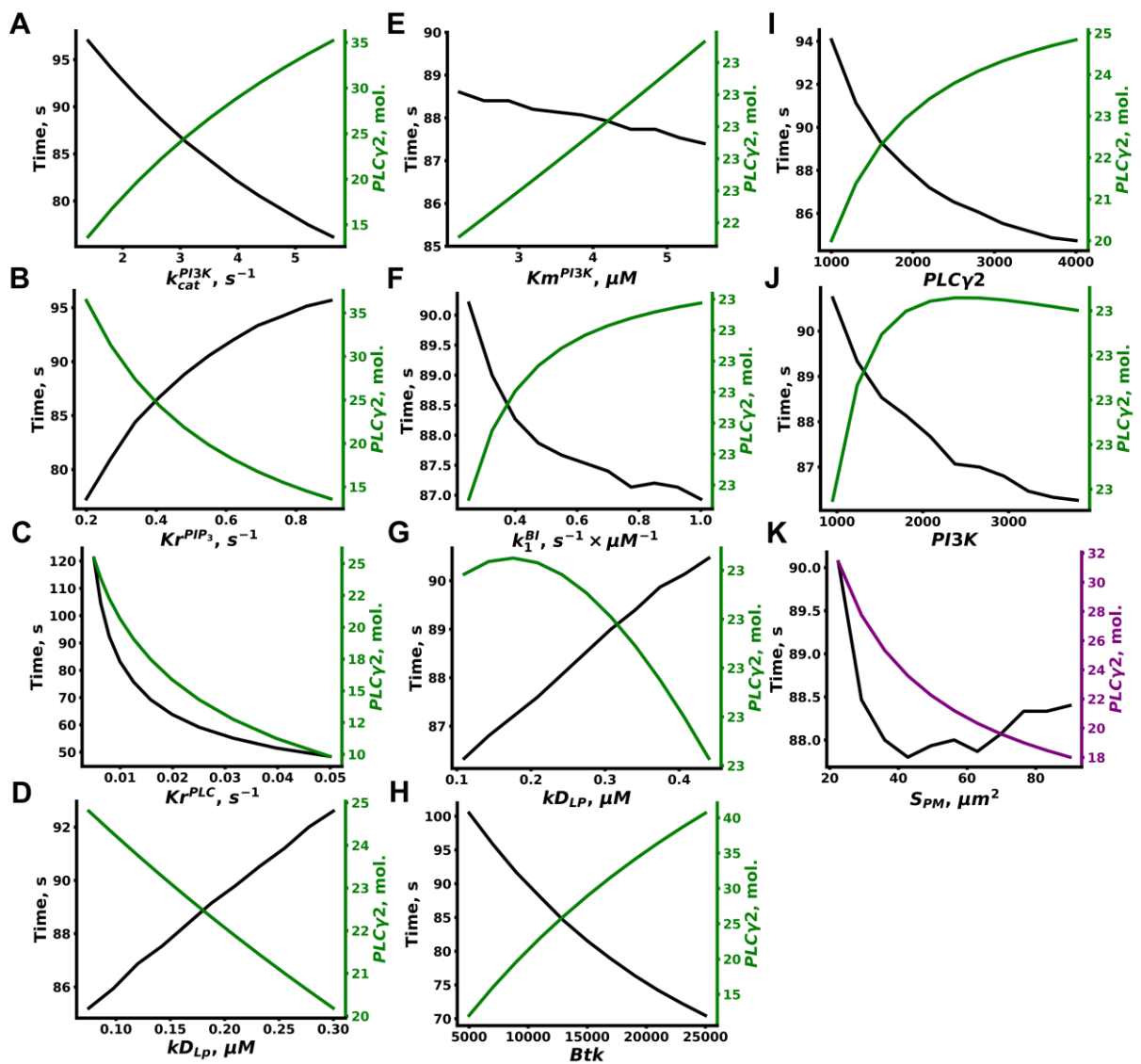
Figure S7. Explicit variation of the parameters with the sensitivity score above 0.01 for effect on maximal amount of active PLCγ2 and time to maximum (from PI3K turnover rate to plasma membrane area). PI3K turnover rate (A), reverse rate of PIP₃ production by PI3K (B), reverse rate of PLCγ2 activation (C), PLCγ2 kD from phosphorylated LAT (D), Michaelis constant of PI3K (E), forward rate of Btk activation upon PIP₃ binding (F), PI3K kD from phosphorylated LAT (G), Btk initial number (H), PLCγ2 initial number (I), PI3K initial number (J), plasma membrane area (K). Green – "LAT-PLCγ2" module, purple – initial volumes of the model compartments.
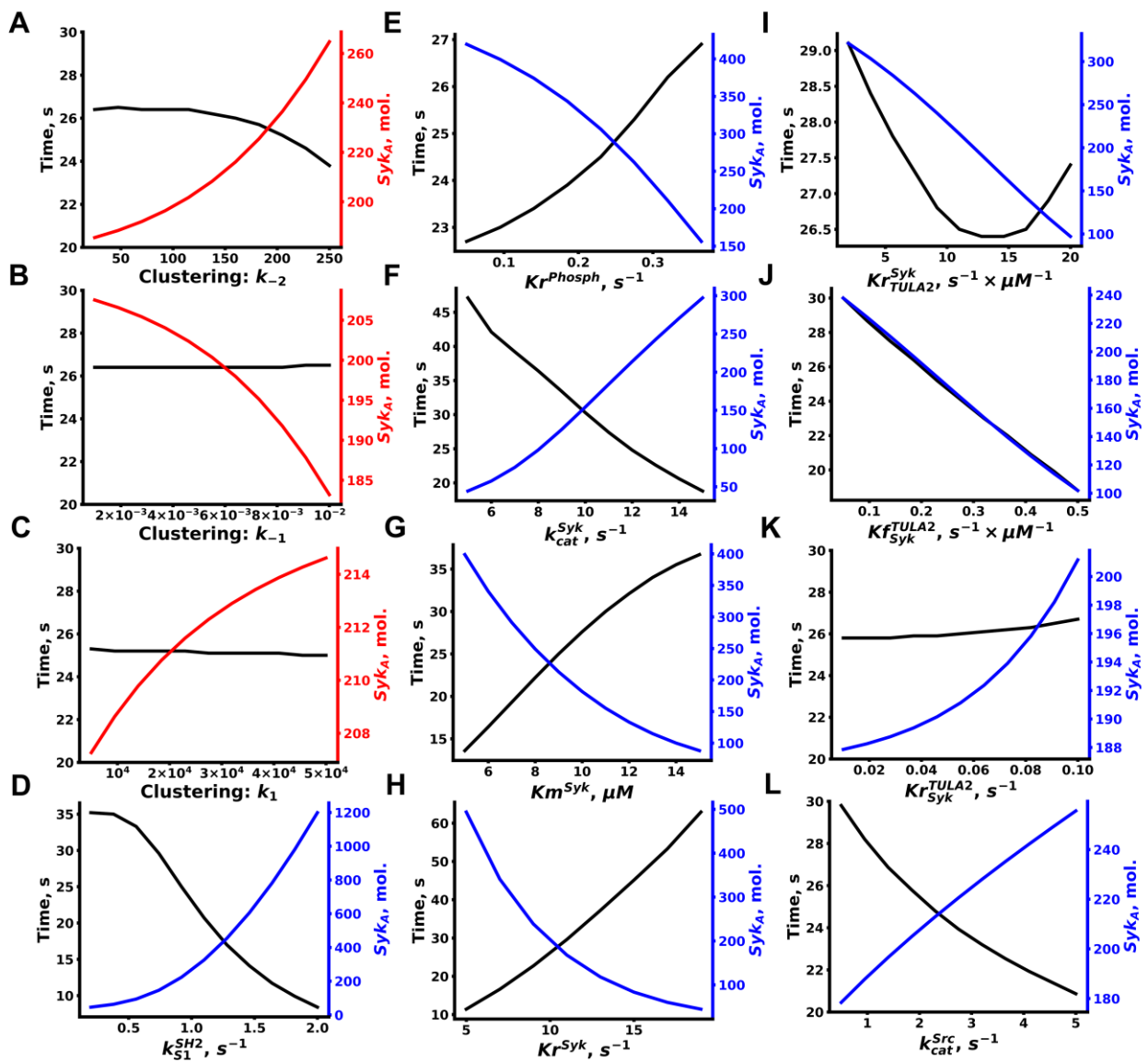
Figure S8. Explicit variation of the parameters with the sensitivity score above 0.01 for effect on maximal amount of active Syk kinases and time to maximum (from CLEC-2 clustering k₋₂ to turnover rate of SFK). CLEC-2 clustering k₋₂ (A), CLEC-2 clustering k₋₁ (B), CLEC-2 clustering k₁ (C), forward rate of Syk activation upon SH-2 domain binding to dually phosphorylated hemITAMs (D), reverse rate of CLEC-2 phosphorylation (E), turnover rate of Syk kinases (F), Michaelis constant of Syk kinases (G), reverse rate of Syk activation by SFK kinases (H), Syk deactivation by TULA-2 rate (I), forward rate of TULA-2 activation by Syk (J), reverse rate of TULA-2 activation by Syk (K), turnover rate of SFK kinases (L). Red colour highlights "CLEC-2 clustering" module, blue – "Tyrosine kinase" module.
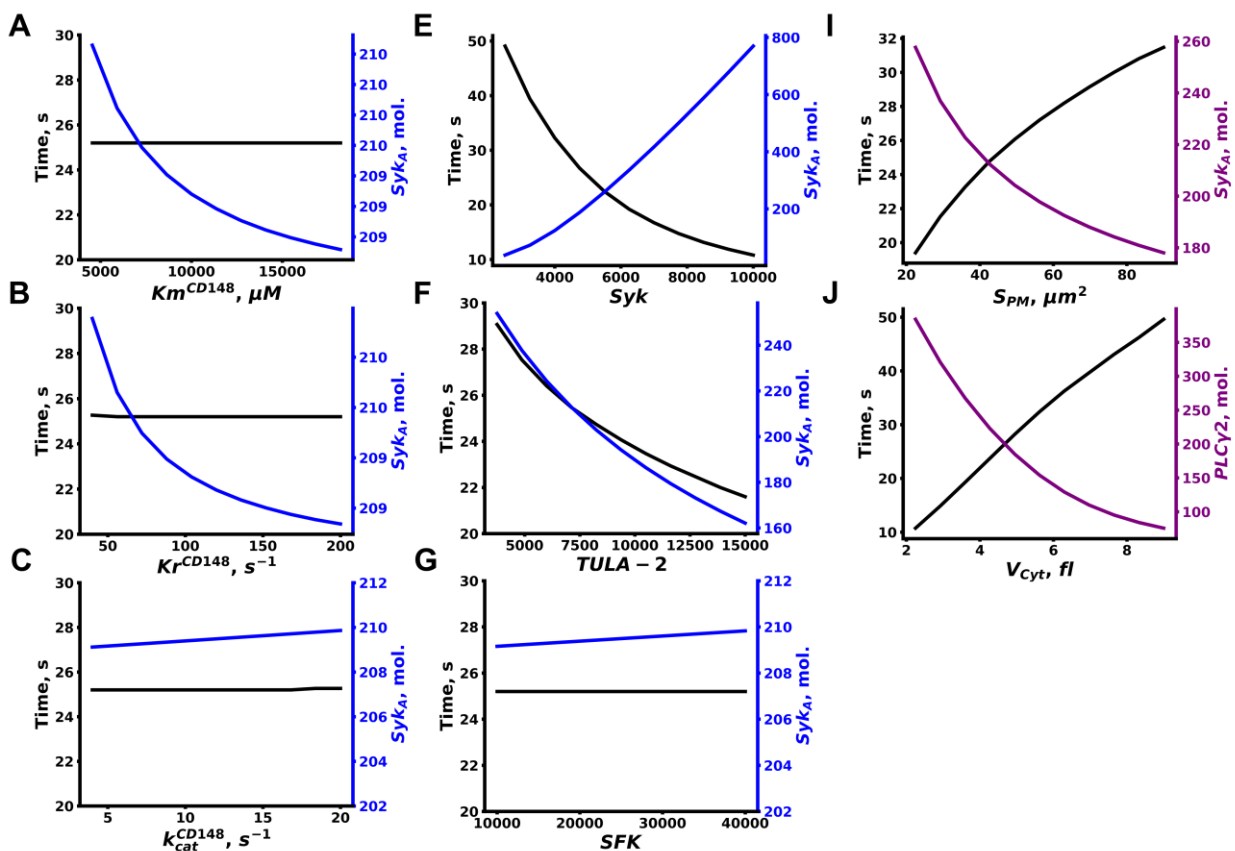
Figure S9. Explicit variation of the parameters with the sensitivity score above 0.01 for effect on maximal amount of active Syk kinases and time to maximum (from Michaelis constant of CD148 to platelet cytosol volume). Michaelis constant of CD148 (A), reverse rate of CD148 activation (B), turnover rate of CD148 (C), Syk initial number (D), TULA-2 initial number (E), SFK initial number (F), plasma membrane area (I), platelet cytosol volume (J). Blue – "Tyrosine kinase" module, purple – initial volumes of the model compartments.
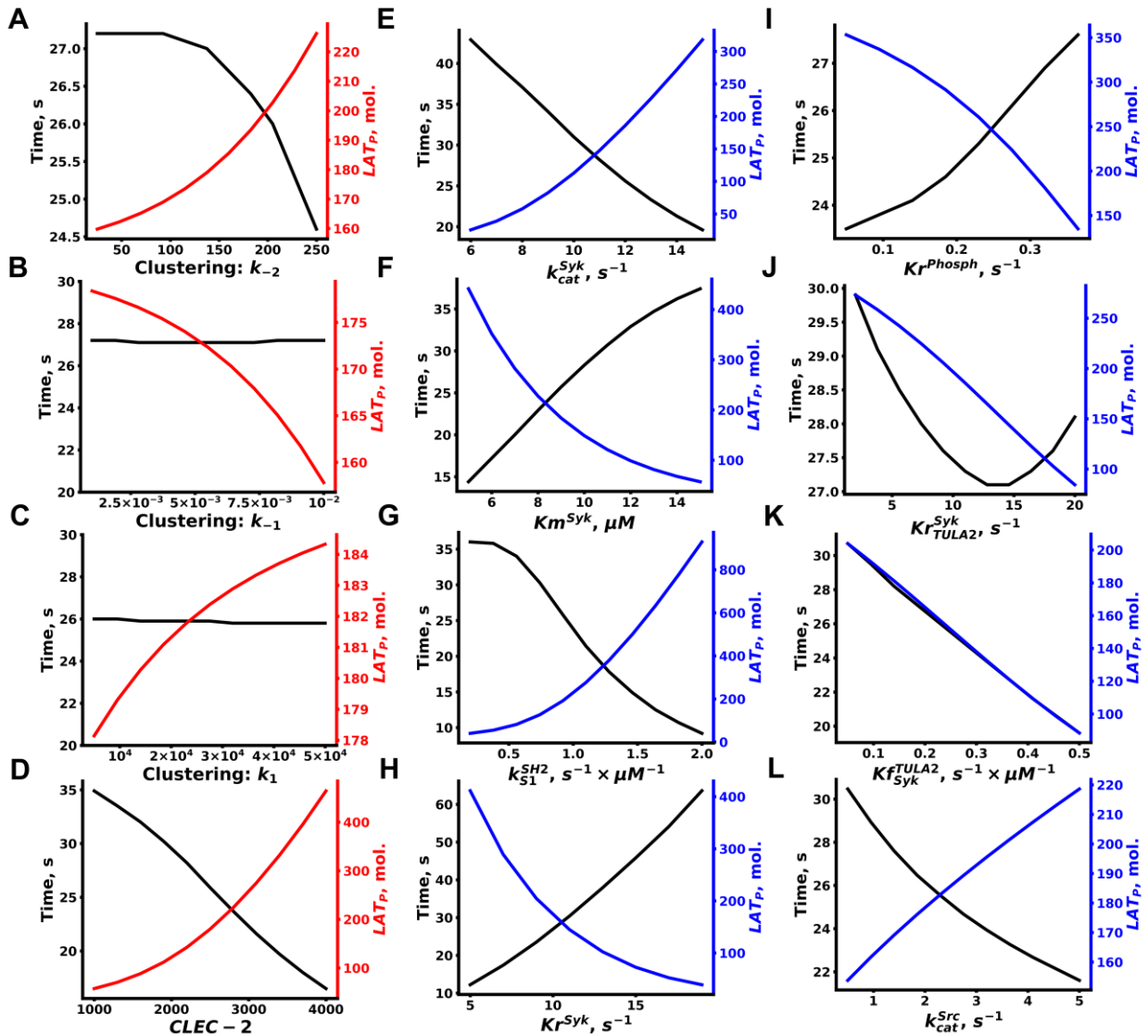
Figure S10. Explicit variation of the parameters with the sensitivity score above 0.01 for effect on maximal amount of phosphorylated LAT and time to maximum (from CLEC-2 clustering k₋₂ to turnover rate of SFK). CLEC-2 clustering k₋₂ (A), CLEC-2 clustering k₋₁ (B), CLEC-2 clustering k₁ (C), CLEC-2 initial number (D), turnover rate of Syk kinases (E), Michaelis constant of Syk kinases (F), forward rate of Syk activation upon SH-2 domain binding to dually phosphorylated hemITAMs (G), reverse rate of Syk activation by SFK kinases (H), reverse rate of CLEC-2 phosphorylation (I), Syk deactivation by TULA-2 rate (J), forward rate of TULA-2 activation by Syk (K), turnover rate of SFK kinases (L). Red colour highlights "CLEC-2 clustering" module, blue – "Tyrosine kinase" module.

Figure S11. Explicit variation of the parameters with the sensitivity score above 0.01 for effect on maximal amount of phosphorylated LAT and time to maximum (from the reverse rate of TULA-2 activation by Syk to plasma membrane area). Reverse rate of TULA-2 activation by Syk (A), Syk SH-2 domains kD from phosphorylated tyrosine residues in hemITAM sequences (B), Syk initial number (C), TULA-2 initial number (D), reverse rate of LAT phosphorylation (F), LAT initial number (G), plasma membrane area (I). Blue – "Tyrosine kinase" module, green – "LAT-PLCγ2" module, purple – initial volumes of the model compartments.
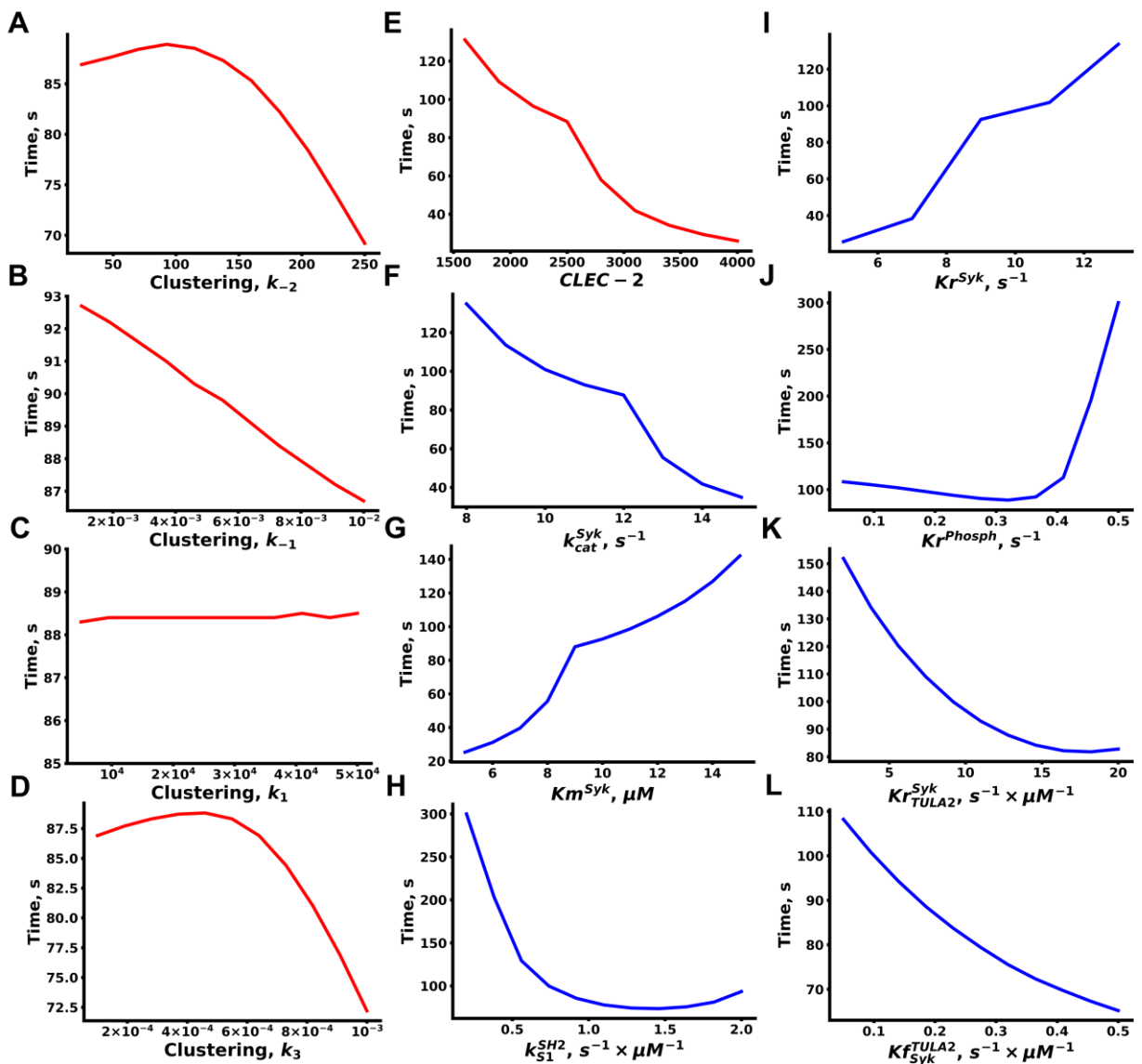
Figure S12. Explicit variation of the parameters with the sensitivity score above 0.01 for effect on the maximal concentration of IP₃ and time to maximum (from CLEC-2 clustering k₋₂ to forward rate of TULA-2 activation by Syk). Inflexion point on the graph corresponds to the initiation of calcium oscillations. CLEC-2 clustering k₋₂ (A), CLEC-2 clustering k₋₁ (B), CLEC-2 clustering k₁ (C), CLEC-2 clustering k₃ (D), CLEC-2 initial number (E), turnover rate of Syk kinases (F), Michaelis constant of Syk kinases (G), forward rate of Syk activation upon SH-2 domain binding to dually phosphorylated hemITAMs (H), reverse rate of Syk activation by SFK kinases (I), reverse rate of CLEC-2 phosphorylation (J), Syk deactivation by TULA-2 rate (K), forward rate of TULA-2 activation by Syk (L). Red colour highlights "CLEC-2 clustering" module, blue – "Tyrosine kinase" module.
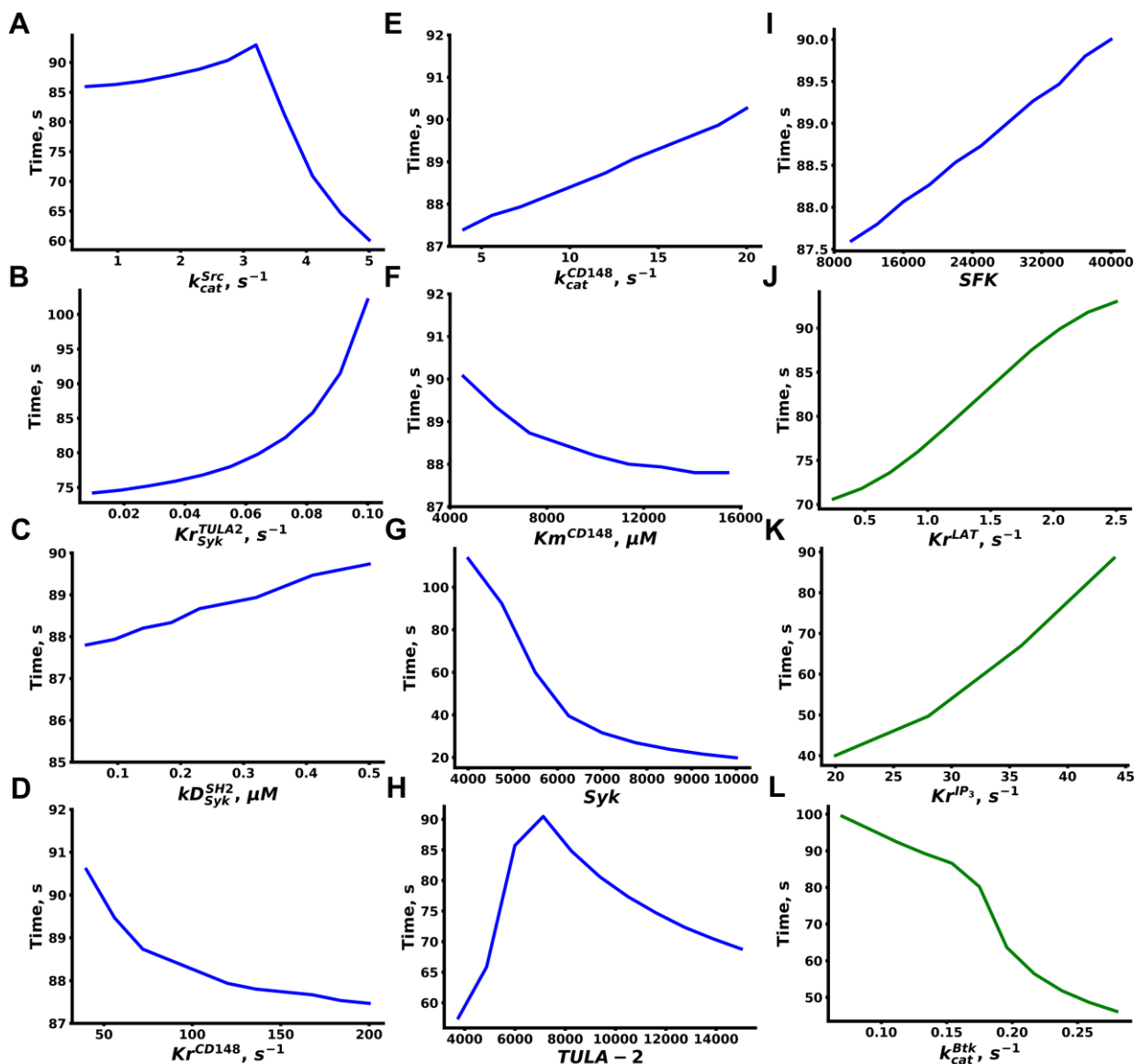
Figure S13. Explicit variation of the parameters with the sensitivity score above 0.01 for effect on the maximal concentration of IP₃ and time to maximum (turnover rate of SFK to turnover rate of Btk). Inflexion point on the graph corresponds to the initiation of calcium oscillations. Turnover rate of SFK (A), reverse rate of TULA-2 activation by Syk (B), Syk SH-2 domains kD from phosphorylated tyrosine residues in hemITAM sequences (C), reverse rate of CD148 activation (D), turnover rate of CD148 (E), Michaelis constant of CD148 (F), Syk initial number (G), TULA-2 initial number (H), SFK initial number (I), reverse rate of LAT phosphorylation (J), reverse rate of IP₃ production (K), turnover rate of Btk (L). Blue – "Tyrosine kinase" module, green – "LAT-PLCγ2" module.
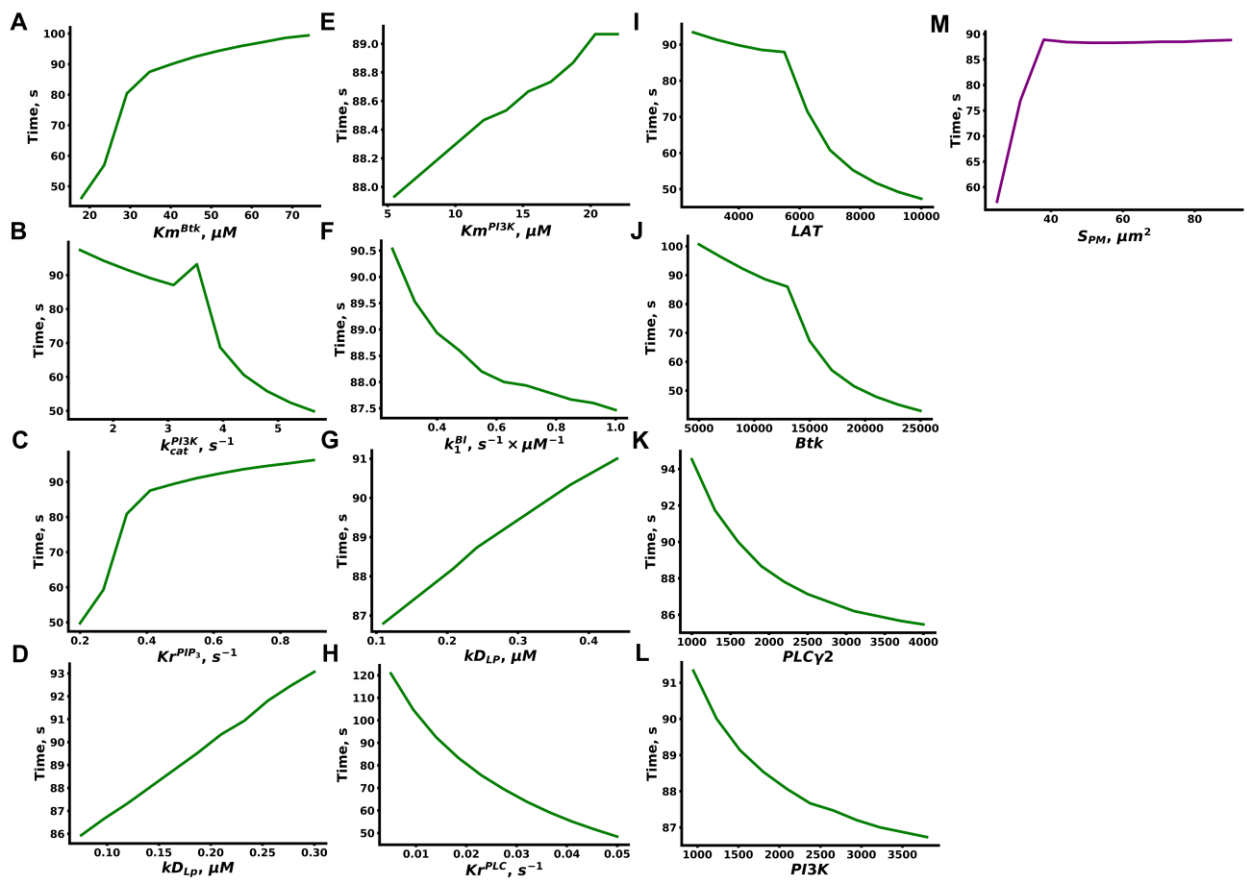
Figure S14. Explicit variation of the parameters with the sensitivity score above 0.01 for effect on the maximal concentration of IP₃ and time to maximum (from Michaelis constant of Btk to plasma membrane area). Inflexion point on the graph corresponds to the initiation of calcium oscillations. Michaelis constant of Btk (A), turnover rate of PI3K (B), reverse rate of PIP₃ production by PI3K (C), PLCγ2 kD from phosphorylated LAT (D), Michaelis constant of PI3K (E), forward rate of Btk activation upon PIP₃ binding (F), PI3K kD from phosphorylated LAT (G), reverse rate of PLCγ2 activation (H), LAT initial number (I), Btk initial number (J), PLCγ2 initial number (K), PI3K initial number (L), plasma membrane area (M). Green – "LAT-PLCγ2" module, purple – initial volumes of the model compartments.
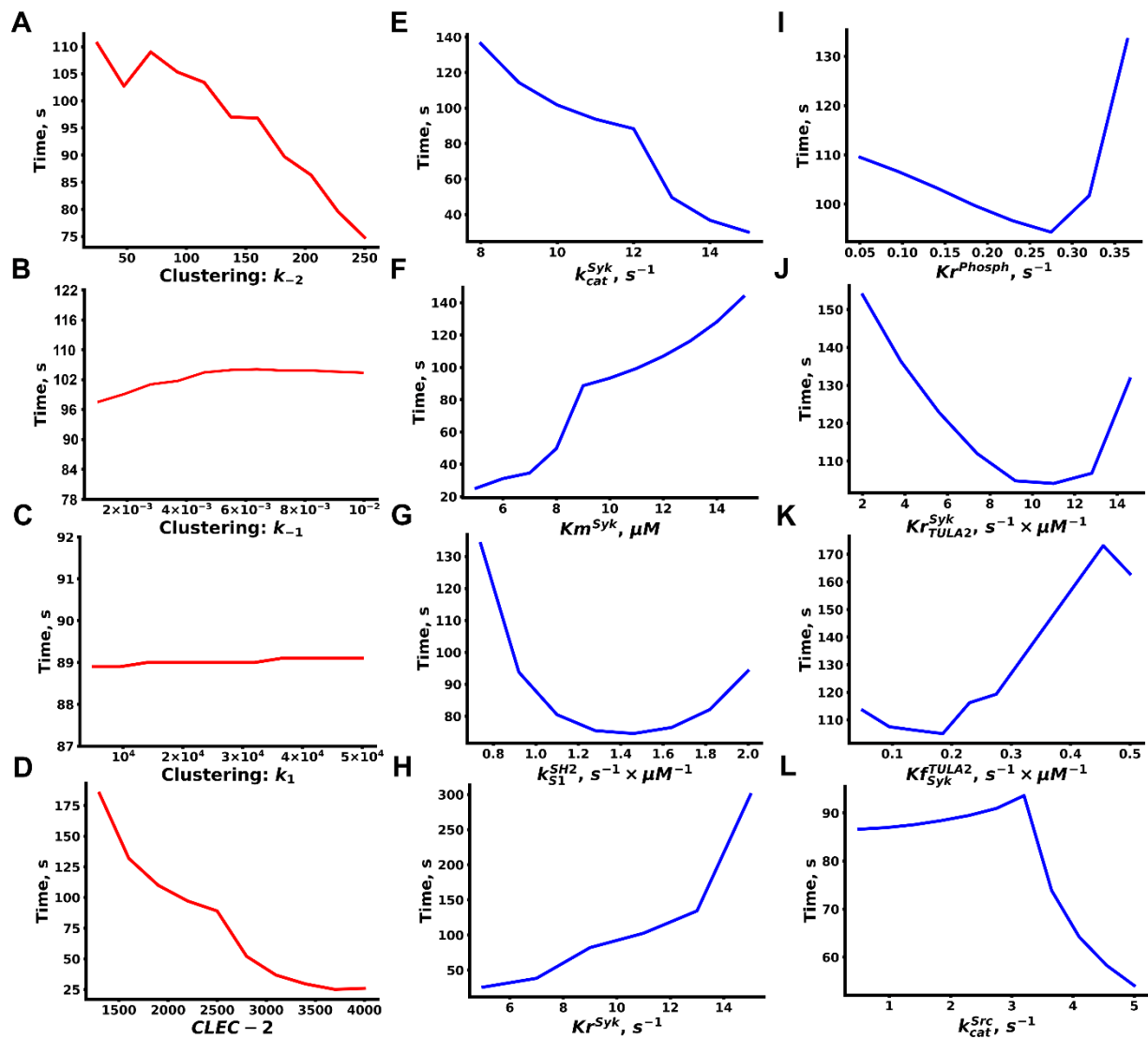
Figure S15. Explicit variation of the parameters with the sensitivity score above 0.01 for effect on the maximal concentration of cytosolic calcium and time to maximum (from CLEC-2 clustering k₋₂ to turnover rate of SFK). **Inflexion point on the graph corresponds to the initiation of calcium oscillations.** CLEC-2 clustering k₋₂ (A), CLEC-2 clustering k₋₁ (B), CLEC-2 clustering k₁ (C), CLEC-2 initial number (D), turnover rate of Syk kinases (E), Michaelis constant of Syk kinases (F), forward rate of Syk activation upon SH-2 domain binding to dually phosphorylated hemITAMs (G), reverse rate of Syk activation by SFK kinases (H), reverse rate of CLEC-2 phosphorylation (I), Syk deactivation by TULA-2 rate (J), forward rate of TULA-2 activation by Syk (K), turnover rate of SFK (L). Red colour highlights "CLEC-2 clustering" module, blue – "Tyrosine kinase" module.
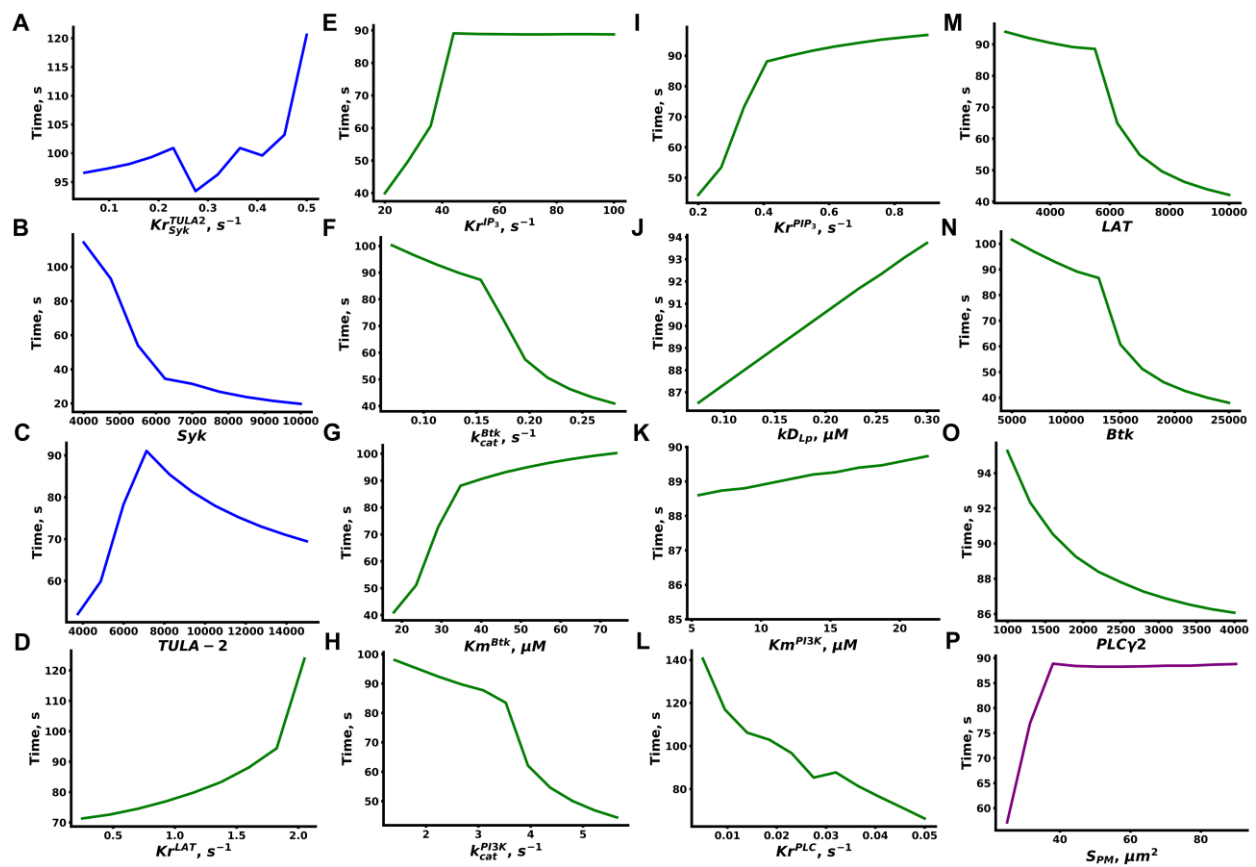
Figure S16. Explicit variation of the parameters with the sensitivity score above 0.01 for effect on the maximal concentration of cytosolic calcium and time to maximum (turnover rate of SFK to turnover rate of Btk). Inflexion point on the graph corresponds to the initiation of calcium oscillations. Reverse rate of TULA-2 activation by Syk (A), Syk initial number (B), TULA-2 initial number (C), reverse rate of LAT phosphorylation (D), reverse rate of IP$_3$ production (E), turnover rate of Btk (F), Michaelis constant of Btk (G), turnover rate of PI3K (H), reverse rate of PIP$_3$ production by PI3K (I), PLCγ2 kD from phosphorylated LAT (D) (J), Michaelis constant of PI3K (K), reverse rate of PLCγ2 activation (L), LAT initial number (M), Btk initial number (N), PLCγ2 initial number (O), plasma membrane area (P).
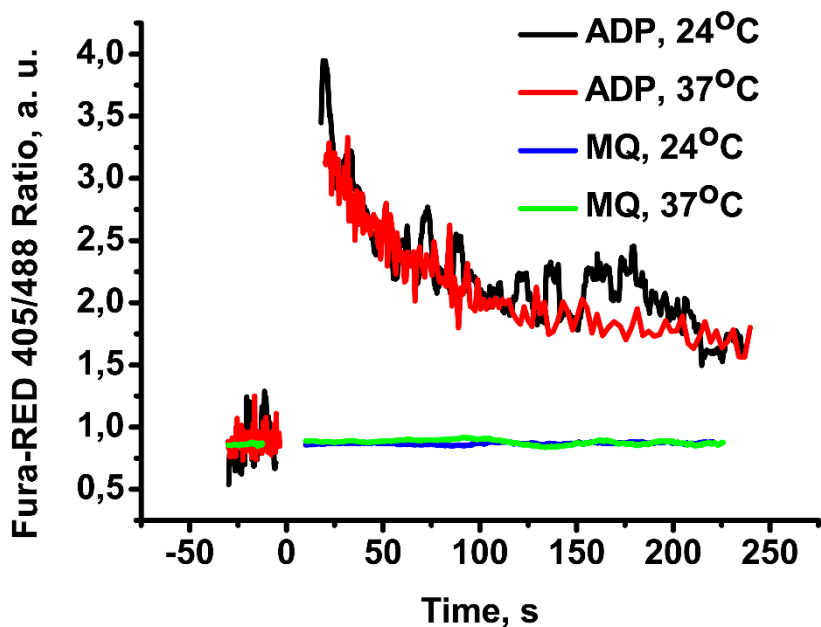
Figure S17. Activation of platelets by 2µM ADP was independent of temperature conditions.
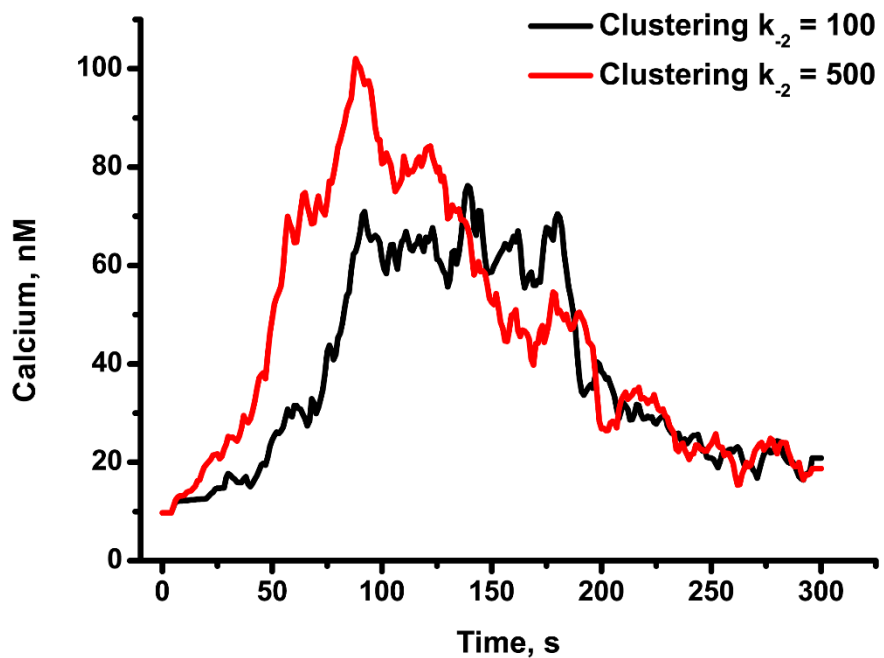

Figure S18. CLEC-2 induced calcium response in platelets, averaged over 100 stochastic runs at different CLEC-2 cluster formation rates.
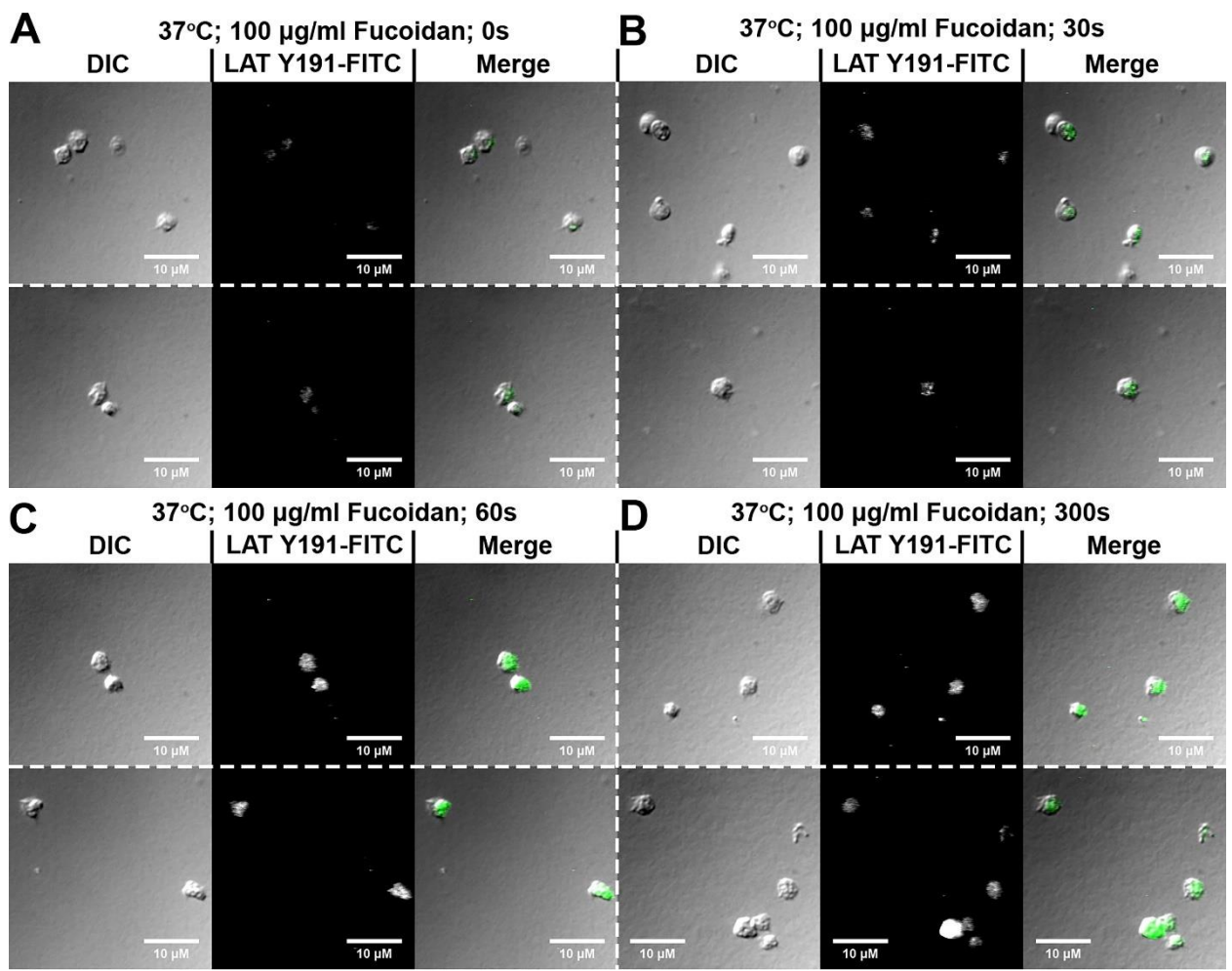
Figure S19. Immunefluorescence of platelets activated by 100 µg/ml Fucoidan at 37°C, fixed at different time-points and stained for phosphorylated LAT. (A) Resting platelets; (B) 30 second incubation with the activator; (C) 60 second incubation with the activator; (D) 300 second incubation with the activator.
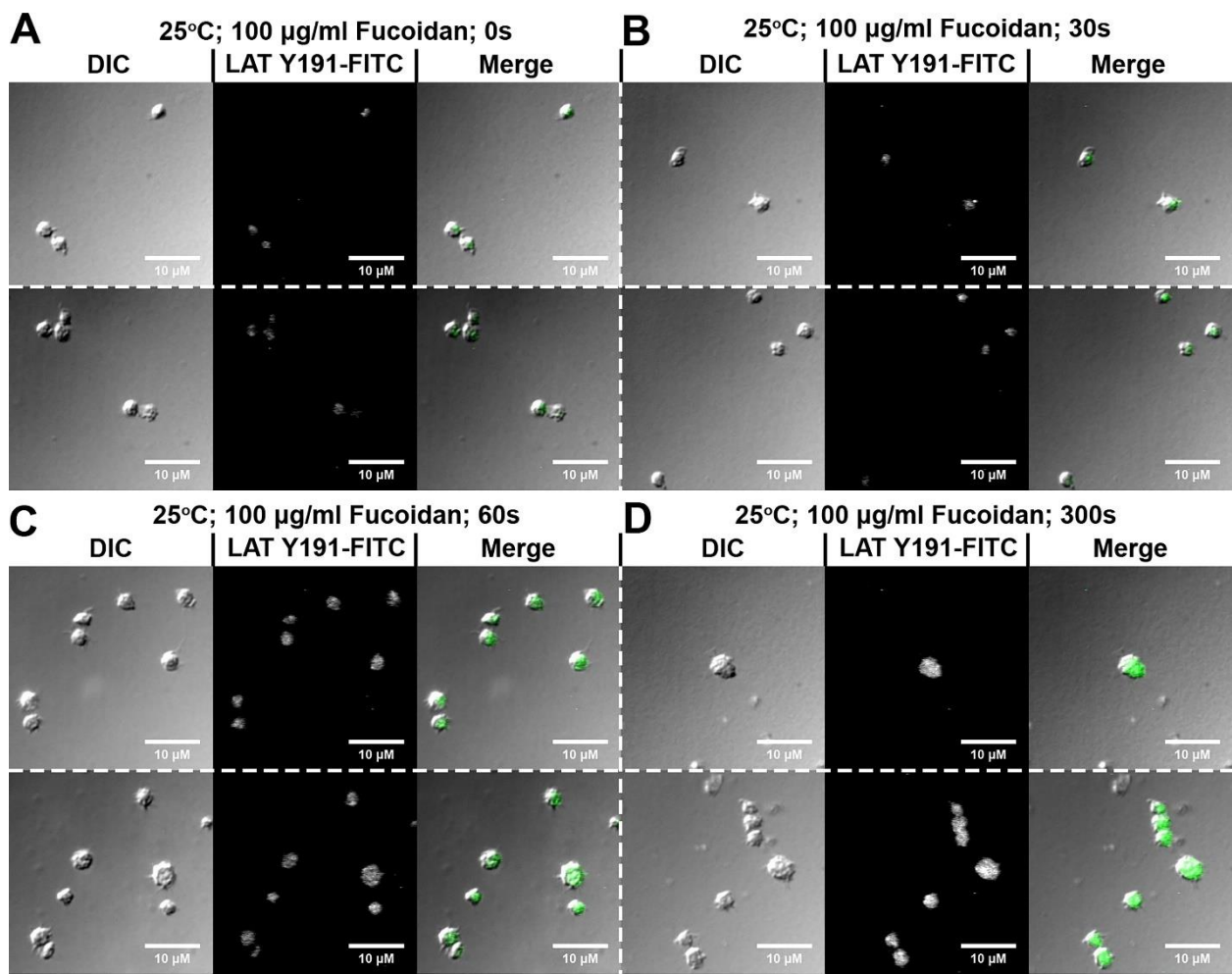
Figure S20. Immunefluorescence of platelets activated by 100 µg/ml Fucoidan at 25°C, fixed at different time-points and stained for phosphorylated LAT. (A) Resting platelets; (B) 30 second incubation with the activator; (C) 60 second incubation with the activator; (D) 300 second incubation with the activator.
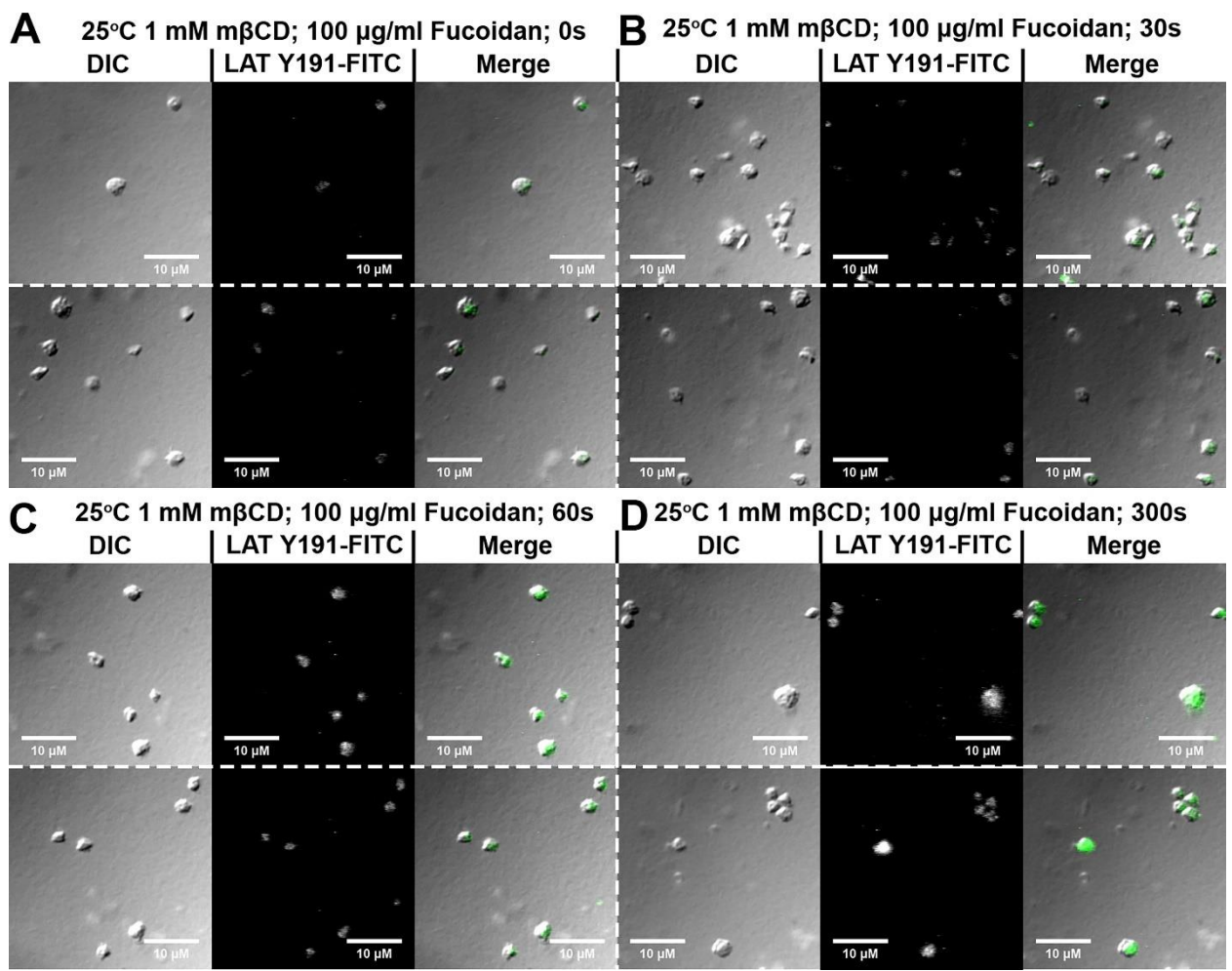
Figure S21. Immunefluorescence of cholesterol depleted platelets activated by 100 µg/ml Fucoidan at 25°C, fixed at different time-points and stained for phosphorylated LAT. (A) Resting platelets; (B) 30 second incubation with the activator; (C) 60 second incubation with the activator; (D) 300 second incubation with the activator.
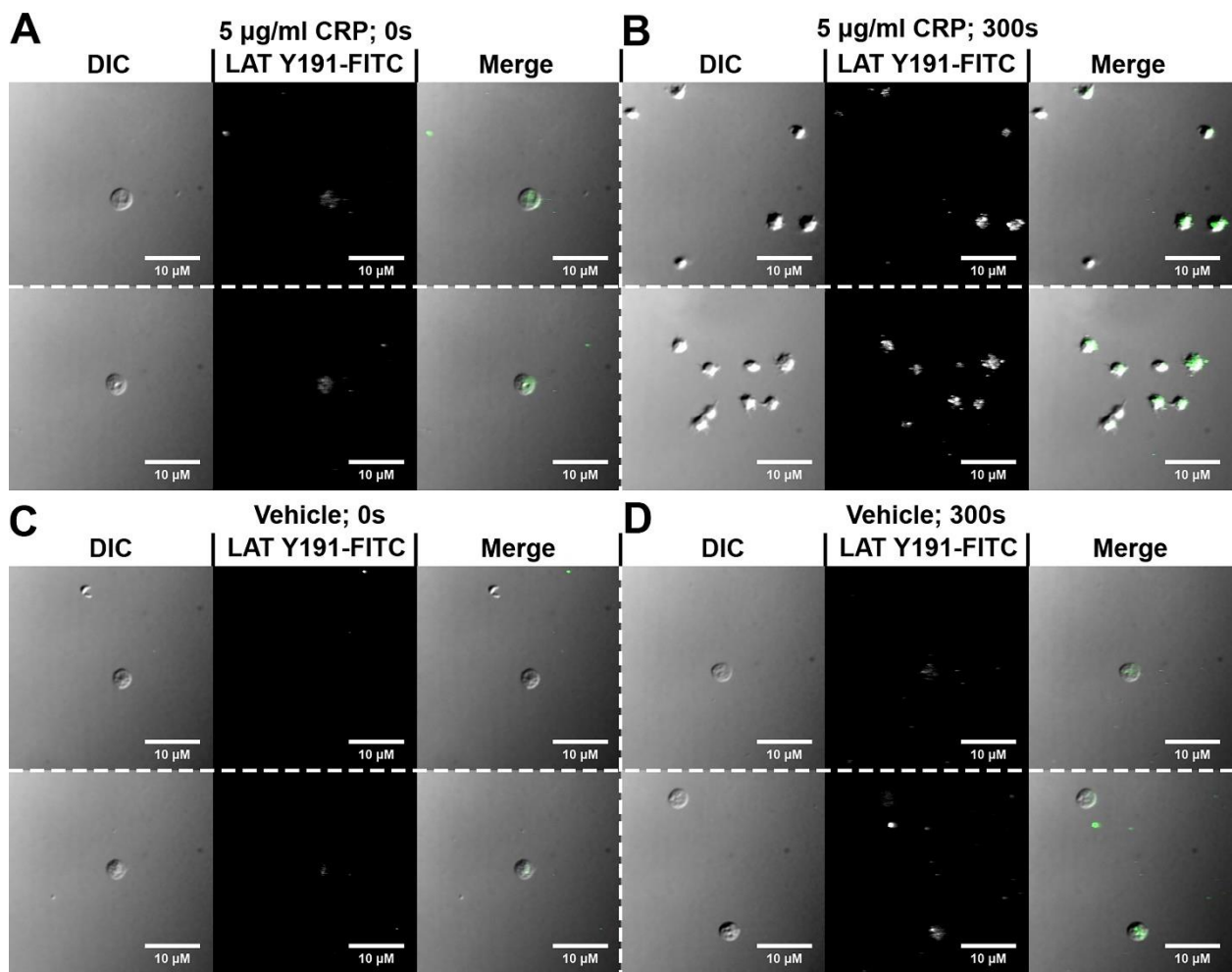
Figure S22. Immunefluorescence of platelets activated either by 5 µg/ml CRP or incubated with MQ, fixed at different time-points and stained for phosphorylated LAT. (A) Resting platelets; (B) 300 second incubation with the activator; (C) resting platelets; (D) 300 second incubation with MQ.

4. Supporting references

1. Mori, J., Y.J. Wang, S. Ellison, S. Heising, B.G. Neel, M.L. Tremblay, S.P. Watson, and Y.A. Senis. 2012. Dominant role of the protein-tyrosine phosphatase CD148 in regulating platelet activation relative to protein-tyrosine phosphatase-1B. Arterioscler. Thromb. Vasc. Biol. 32: 2956–2965.

2. Senis, Y.A., A. Mazharian, and J. Mori. 2014. Src family kinases: at the forefront of platelet activation. Blood. 124: 2013–2024.

3. Coxon, C.H., M.J. Geer, and Y.A. Senis. 2017. ITIM receptors: More than just inhibitors of platelet activation. Blood. 129: 3407–3418.

4. Bradshaw, J.M. 2010. The Src, Syk, and Tec family kinases: Distinct types of molecular switches. Cell. Signal. 22: 1175–1184.

5. Tiganis, T., and A.M. Bennett. 2007. Protein tyrosine phosphatase function: the substrate perspective. Biochem. J. 402: 1 LP – 15.

6. Spring, K., C. Chabot, S. Langlois, L. Lapointe, N.T.N. Trinh, C. Caron, J.K. Hebda, J. Gavard, M. Elchebly, and I. Royal. 2012. Tyrosine phosphorylation of DEP-1/CD148 as a mechanism controlling Src kinase activation, endothelial cell permeability, invasion, and capillary formation. Blood. 120: 2745–2756.

7. Rathore, V.B., M. Okada, P.J. Newman, and D.K. Newman. 2007. Paxillin family members function as Csk-binding proteins that regulate Lyn activity in human and murine platelets. Biochem. J. 403: 275–281.

8.   Lin, X., S. Lee, and G. Sun. 2003. Functions of the activation loop in Csk protein-tyrosine kinase. J. Biol. Chem. 278: 24072–24077.

9.   Hughes, C.E., B.A. Finney, F. Koentgen, K.L. Lowe, and S.P. Watson. 2015. The N-terminal SH2 domain of Syk is required for (hem) ITAM , but not integrin , signaling in mouse platelets. Blood. 125: 144–155.

10. Severin, S., A.Y. Pollitt, L. Navarro-Nunez, C.A. Nash, D. Mour??o-S??, J.A. Eble, Y.A. Senis, and S.P. Watson. 2011. Syk-dependent phosphorylation of CLEC-2: A novel mechanism of hem-immunoreceptor tyrosine-based activation motif signaling. J. Biol. Chem. 286: 4107–4116.

11. Garzon Dasgupta, A.K., A.A. Martyanov, A.A. Filkova, M.A. Panteleev, and A.N. Sveshnikova. 2020. Development of a simple kinetic mathematical model of aggregation of proteins or clustering of receptors. Submiss. .

12. Pollitt, A.Y., N.S. Poulter, E. Gitz, L. Navarro-Nuñez, Y.J. Wang, C.E. Hughes, S.G. Thomas, B. Nieswandt, M.R. Douglas, D.M. Owen, D.G. Jackson, M.L. Dustin, and S.P. Watson. 2014. Syk and src family kinases regulate c-type lectin receptor 2 (clec-2)-mediated clustering of podoplanin and platelet adhesion to lymphatic endothelial cells. J. Biol. Chem. 289: 35695–35710.

13. Filkova, A.A., A.A. Martyanov, A.K. Garzon Dasgupta, M.A. Panteleev, and A.N. Sveshnikova. 2019. Quantitative dynamics of reversible platelet aggregation: mathematical modelling and experiments. Sci. Rep. 9: 6217.

14. Manne, B.K., T.M. Getz, C.E. Hughes, O. Alshehri, C. Dangelmaier, U.P. Naik, S.P. Watson, and S.P. Kunapuli. 2013. Fucoidan is a novel platelet agonist for the C-type lectin-like receptor 2 (CLEC-2). J. Biol. Chem. 288: 7717–7726.

15. Musumeci, L., M.J. Kuijpers, K. Gilio, A. Hego, E. Th????tre, L. Maurissen, M. Vandereyken, C. V. Diogo, C. Lecut, W. Guilmain, E. V. Bobkova, J.A. Eble, R. Dahl, P. Drion, J. Rascon, Y. Mostofi, H. Yuan, E. Sergienko, T.D.Y. Chung, M. Thiry, Y. Senis, M. Moutschen, T. Mustelin, P. Lancellotti, J.W.M. Heemskerk, L. Tautz, C. Oury, and S. Rahmouni. 2015. Dual-specificity phosphatase 3 deficiency or inhibition limits platelet activation and arterial thrombosis. Circulation. 131: 656–668.

16. Sveshnikova, A.N., A. V. Balatskiy, A.S. Demianova, T.O. Shepelyuk, S.S. Shakhidzhanov, M.N. Balatskaya, A. V. Pichugin, F.I. Ataullakhanov, and M.A. Panteleev. 2016. Systems biology insights into the meaning of the platelet's dual-receptor thrombin signaling. J. Thromb. Haemost. 14: 2045–2057.

17. Balabin, F.A., and A.N. Sveshnikova. 2016. Computational biology analysis of platelet signaling reveals roles of feedbacks through phospholipase C and inositol 1,4,5-trisphosphate 3-kinase in controlling amplitude and duration of calcium oscillations. Math. Biosci. 276: 67–74.

18. Dunster, J.L., F. Mazet, M.J. Fry, J.M. Gibbins, and M.J. Tindall. 2015. Regulation of Early Steps of GPVI Signal Transduction by Phosphatases: A Systems Biology Approach. PLoS Comput. Biol. 11: 1–26.

19. Sveshnikova, A.N., F.I. Ataullakhanov, and M.A. Panteleev. 2015. Compartmentalized calcium signaling triggers subpopulation formation upon platelet activation through PAR1. Mol. BioSyst. 11: 1052–1060.

20. Eckly, A., J.Y. Rinckel, F. Proamer, N. Ulas, S. Joshi, S.W. Whiteheart, and C. Gachet. 2016. Respective contributions of single and compound granule fusion to secretion by activated platelets. Blood. 128: 2538–2549.

21. Gitz, E., A.Y. Pollitt, J.J. Gitz-Francois, O. Alshehri, J. Mori, S. Montague, G.B. Nash, M.R. Douglas, E.E. Gardiner, R.K. Andrews, C.D. Buckley, P. Harrison, and S.P. Watson. 2014. CLEC-2 expression is maintained on activated platelets and on platelet microparticles. Blood. 124: 2262–2270.

22. Burkhart, J.M., M. Vaudel, S. Gambaryan, S. Radau, U. Walter, L. Martens, J. Geiger, A. Sickmann, and R.P. Zahedi. 2012. The first comprehensive and quantitative analysis of human platelet protein composition allows the comparative analysis of structural and functional pathways. Blood. 120.

23. Kemble, D.J., Y.H. Wang, and G. Sun. 2006. Bacterial expression and characterization of catalytic loop mutants of Src protein tyrosine kinase. Biochemistry. 45: 14749–14754.

24. Ren, L., X. Chen, R. Luechapanichkul, N.G. Selner, T.M. Meyer, A.-S. Wavreille, R. Chan, C. Iorio, X. Zhou, B.G. Neel, and D. Pei. 2011. Substrate Specificity of Protein Tyrosine Phosphatases 1B, RPTPα, SHP-1, and SHP-2.

Biochemistry. 50: 2339–2356.

25. Park, M.J., R. Sheng, A. Silkov, D.J. Jung, Z.G. Wang, Y. Xin, H. Kim, P. Thiagarajan-Rosenkranz, S. Song, Y. Yoon, W. Nam, I. Kim, E. Kim, D.G. Lee, Y. Chen, I. Singaram, L. Wang, M.H. Jang, C.S. Hwang, B. Honig, S. Ryu, J. Lorieau, Y.M. Kim, and W. Cho. 2016. SH2 Domains Serve as Lipid-Binding Modules for pTyr-Signaling Proteins. Mol. Cell. 62: 7–20.

26. Tsang, E., A.M. Giannetti, D. Shaw, M. Dinh, J.K.Y. Tse, S. Gandhi, A. Ho, S. Wang, E. Papp, and J.M. Bradshaw. 2008. Molecular mechanism of the Syk activation switch. J. Biol. Chem. 283: 32650–32659.

27. Hughes, C.E., U. Sinha, A. Pandey, J.A. Eble, C.A. O'Callaghan, and S.P. Watson. 2013. Critical role for an acidic amino acid region in platelet signaling by the HemITAM (hemi-immunoreceptor tyrosine-based activation motif) containing receptor CLEC-2 (C-type lectin receptor-2). J. Biol. Chem. 288: 5127–5135.

28. Dinh, M., D. Grunberger, H. Ho, S.Y. Tsing, D. Shaw, S. Lee, J. Barnett, R.J. Hill, D.C. Swinney, and J.M. Bradshaw. 2007. Activation Mechanism and Steady State Kinetics of Bruton's Tyrosine Kinase. J. Biol. Chem. 282: 8768–8776.

29. Hughes, C.E., A.Y. Pollitt, J. Mori, J.A. Eble, M.G. Tomlinson, J.H. Hartwig, C.A. O'Callaghan, K. Fütterer, and S.P. Watson. 2010. CLEC-2 activates Syk through dimerization. Blood. 115: 2947–2955.